

# Inertial effects in nonequilibrium work fluctuations by a path integral approach

Tooru Taniguchi and E. G. D. Cohen

*The Rockefeller University, 1230 York Avenue, New York, NY 10021, USA.*

(Dated: February 1, 2008)

Inertial effects in fluctuations of the work to sustain a system in a nonequilibrium steady state are discussed for a dragged massive Brownian particle model using a path integral approach. We calculate the work distribution function in the laboratory and comoving frames and prove the asymptotic fluctuation theorem for these works for any initial condition. Important and observable differences between the work fluctuations in the two frames appear for finite times and are discussed concretely for a nonequilibrium steady state initial condition. We also show that for finite times a time oscillatory behavior appears in the work distribution function for masses larger than a nonzero critical value.

PACS numbers: 05.70.Ln, 05.40.-a, 05.10.Gg

## I. INTRODUCTION

In recent years, fluctuations in nonequilibrium systems have drawn considerable attention to a new kind of fluctuation theorems. These fluctuation theorems are asymmetric relations for the distribution functions for work, heat, etc., and may be satisfied even far from equilibrium states or for small systems in which the magnitude of the fluctuations can be large. These fluctuation theorems have been proved for deterministic thermostated systems [1, 2, 3] as well as for stochastic systems [4, 5], and have also been discussed in connection with the Onsager-Machlup fluctuation theory [6]. Moreover, experimental confirmations for these theorems have been obtained [9, 10, 11, 12]. It has also been shown that the fluctuation theorems include the fluctuation-dissipation theorem, as well as Onsager's reciprocal relations, near equilibrium states [1, 5, 13].

In our previous paper [6], based on a generalization of the Onsager-Machlup theory for fluctuations around equilibrium to those around nonequilibrium steady states using a path integral approach, we discussed fluctuation theorems for a stochastic dynamics described by a Langevin equation. For a Brownian particle driven by a mechanical force  $F(x_s, s)$ , the Langevin equation for the particle position  $x_s$  at time  $s$  is of the general form

$$m \frac{d^2 x_s}{ds^2} = -\alpha \frac{dx_s}{ds} + F(x_s, s) + \zeta_s \quad (1)$$

with the mass  $m$  of the particle, the friction coefficient  $\alpha$  and a random noise  $\zeta_s$ . In our previous paper, as a nonequilibrium model we considered a dragged Brownian particle, in which the mechanical force is given by a harmonic force  $F(x_s, s) = -\kappa(x_s - v s)$  with the spring constant  $\kappa$  and the dragging velocity  $v$ . Furthermore we mainly considered this model under the over-damped assumption. This assumption can be used for a dynamics on a much longer time scale than the inertial characteristic time  $\tau_m \equiv m/\alpha$ , and the dynamical equation under this assumption is simply given by neglecting the inertial

term containing the mass in Eq. (1), i.e. by

$$\frac{dx_s}{ds} = \frac{1}{\alpha} F(x_s, s) + \frac{1}{\alpha} \zeta_s. \quad (2)$$

Equation (2) is much simpler than Eq. (1), but information of the system on the shorter time scale than  $\tau_m$  is lost in Eq. (2). It may be noted that Machlup and Onsager already developed their fluctuation theory around equilibrium not only for the case corresponding to the over-damped case [7] but also for the inertial case [8]. In our previous paper we discussed also a generalization of the Onsager-Machlup theory for nonequilibrium steady states including the inertial term [6]. However, there we treated only one type of fluctuation theorem, the so called transient fluctuation theorem [2], which is restricted to equilibrium initial conditions. Another fluctuation theorem, the asymptotic fluctuation theorem [3], which holds for any initial condition (including a nonequilibrium steady state[24]), was not discussed for inertial cases in Ref. [6]. Different from the transient fluctuation theorem, which is correct for all times as a mathematical identity [14], the asymptotic fluctuation theorem is satisfied in the long time limit only. However, as we will discuss in this paper, a variety of interesting inertial effects appear for finite times for a nonequilibrium initial condition, before the asymptotic fluctuation theorem is achieved. Although there are some results for fluctuation theorems for stochastic systems including inertia [15, 16], the asymptotic fluctuation theorem with inertia has not been discussed fully in connection with the Onsager-Machlup theory so far.

The purpose of this paper is therefore to discuss, in the context of the Onsager-Machlup path integral approach, inertial effects in nonequilibrium steady state work fluctuations, including the asymptotic fluctuation theorem. For these discussions we use the Langevin equation (1) for a dragged Brownian particle without the over-damped assumption. The work distribution function is calculated explicitly for any initial condition, and its finite time properties are investigated. As an important inertial effect we show a critical value of mass above which the work distribution function shows a time-oscillatory

behavior.

The nonequilibrium work used in this paper is based on the generalized Onsager-Machlup theory, as obtained in our previous paper [6]. In that paper we considered two kinds of work in two different frames: (A) the work  $\mathcal{W}_l$  done in the laboratory frame ( $l$ ) and (B) the work  $\mathcal{W}_c$  done in the comoving frame ( $c$ ) where the average velocity of the Brownian particle is zero in a nonequilibrium steady state. A difference between these two works is that  $\mathcal{W}_c$  includes a d'Alembert-like force, which is absent in  $\mathcal{W}_l$ . In this paper, we show that both the works  $\mathcal{W}_l$  and  $\mathcal{W}_c$  satisfy the asymptotic fluctuation theorem. We also discuss dramatic differences between the work distribution functions for  $\mathcal{W}_l$  and  $\mathcal{W}_c$  for finite times.

The outline of this paper is as follows. In Sec. II we introduce a dragged Brownian particle model with inertia, and treat its dynamics using a path integral. In Sec. III we introduce the works done in the laboratory and comoving frames and calculate their distribution functions. In Sec. IV we prove the asymptotic work fluctuation theorem. In Sec. V we discuss inertial effects in the work distribution functions for finite times. Finally, Sec. VI is devoted to a summary and some remarks on this paper.

## II. DRAGGED BROWNIAN PARTICLE WITH INERTIA

We consider a Brownian particle confined by a harmonic potential, which moves with a constant velocity  $v$  through a fluid, as discussed in our previous paper [6]. The dynamics of this particle is described by a Langevin equation

$$m \frac{d^2 x_s}{ds^2} = -\alpha \frac{dx_s}{ds} - \kappa (x_s - vs) + \zeta_s. \quad (3)$$

Here, we assume that  $\zeta_s$  is the Gaussian-white random force whose probability functional  $P_\zeta(\{\zeta_s\})$  for  $\{\zeta_s\}_{s \in [t_0, t]}$  is given by

$$P_\zeta(\{\zeta_s\}) = C_\zeta \exp \left( -\frac{\beta}{4\alpha} \int_{t_0}^t ds \zeta_s^2 \right) \quad (4)$$

with the normalization coefficient  $C_\zeta$  and the inverse temperature  $\beta \equiv 1/(k_B T)$ , where  $k_B$  is the Boltzmann's constant and  $T$  is the temperature of the heat reservoir. [Note that the coefficient  $C_\zeta$  can depend on the initial time  $t_0$  and the final time  $t$ , but such time dependences in  $C_\zeta$ , as well as in similar coefficients  $C_x$  and  $C_\mathcal{E}$  introduced later, are suppressed.] It follows from Eq. (4) that the first two auto-correlation functions of the random force  $\zeta_s$  are given by  $\langle \zeta_s \rangle = 0$  and  $\langle \zeta_{s_1} \zeta_{s_2} \rangle = (2\alpha/\beta) \delta(s_1 - s_2)$  with the notation  $\langle \cdots \rangle$  for an initial ensemble average.

Now, we consider the probability functional  $P_x(\{x_s\})$  for a path  $\{x_s\}_{s \in [t_0, t]}$  of the particle position  $x_s$ . By inserting Eq. (3) into Eq. (4) and interpreting the probability functional  $P_\zeta(\{\zeta_s\})$  for  $\zeta_s$  as the probability func-

tional  $P_x(\{x_s\})$  for  $x_s$ , we obtain, apart from a normalization coefficient,

$$P_x(\{x_s\}) = C_x \exp \left[ -\frac{1}{4D} \int_{t_0}^t ds \left( \dot{x}_s + \frac{x_s - vs}{\tau_r} + \frac{m}{\alpha} \ddot{x}_s \right)^2 \right] \quad (5)$$

with  $\dot{x}_s \equiv dx_s/ds$ ,  $\ddot{x}_s \equiv d^2 x_s/ds^2$  and the normalization coefficient  $C_x$ . Here,  $D \equiv k_B T/\alpha$  is the diffusion constant given by the Einstein relation and  $\tau_r \equiv \alpha/\kappa$  is the relaxation time in the over-damped case. For another derivation of Eq. (5) via a Fokker-Planck equation corresponding to the Langevin equation, see, for example, Ref. [17].

For systems whose dynamics is expressed by a second-order Langevin equation, like Eq. (3), we introduce the path integration of any functional  $X(\{x_s\})$  as  $\int_{(x_{t_0}, \dot{x}_{t_0})=(x_i, p_i/m)}^{(x_t, \dot{x}_t)=(x_f, p_f/m)} \mathcal{D}x_s X(\{x_s\})$ , with respect to paths  $\{x_s\}_{s \in (t_0, t)}$  satisfying the initial ( $i$ ) condition  $(x_{t_0}, \dot{x}_{t_0}) = (x_i, p_i/m)$  and the final ( $f$ ) condition  $(x_t, \dot{x}_t) = (x_f, p_f/m)$ . Using this notation for the functional integral, the functional average  $\langle X(\{x_s\}) \rangle_t$  over all possible paths  $\{x_s\}_{s \in (t_0, t)}$ , as well as averages over the initial and final positions and momenta of the particle is represented by

$$\begin{aligned} \langle X(\{x_s\}) \rangle_t &\equiv \iint dx_i dp_i \int_{(x_{t_0}, \dot{x}_{t_0})=(x_i, p_i/m)}^{(x_t, \dot{x}_t)=(x_f, p_f/m)} \mathcal{D}x_s \\ &\quad \times \int \int dx_f dp_f X(\{x_s\}) \\ &\quad \times P_x(\{x_s\}) f(x_i, p_i, t_0) \end{aligned} \quad (6)$$

with the initial distribution function  $f(x_i, p_i, t_0)$  for the particle position  $x_i$  and momentum  $p_i$ . The normalization condition to specify the coefficient  $C_x$  of the distribution functional (5) is given by  $\langle 1 \rangle_t = 1$  using the notation (6) as well as the normalization condition  $\iint dx_i dp_i f(x_i, p_i, t_0) = 1$  for the initial distribution function  $f(x_i, p_i, t_0)$ .

This finishes the introduction of our model and its dynamics. In the next section III we introduce the work done on this system and calculate its probability distribution.

## III. WORK DISTRIBUTION

### A. Work to Drag a Brownian Particle and its Distribution

In our previous paper [6], we considered the work  $\mathcal{W}$  to move the confining potential with a velocity  $v$  in two frames; the laboratory frame using the particle position  $x_s$  and the comoving frame using the particle position  $y_s \equiv x_s - vs$  at time  $s$ . Based on a generalized Onsager-Machlup theory, we showed in Ref. [6] that the work  $\mathcal{W}_l$

done in the laboratory frame is given by  $\int_{t_0}^t ds [-\kappa(x_s - vs)]v$ , and the work  $\mathcal{W}_c$  done in the comoving frame is given by  $\int_{t_0}^t ds (-\kappa y_s - m\ddot{y}_s)v$  with  $\ddot{y}_s \equiv d^2 y_s / ds^2 = \ddot{x}_s$ , leading to a difference between the work  $\mathcal{W}$  in these two frames by an inertial or d'Alembert-like force  $-m\ddot{y}_s$ . To understand this difference in a concise way, note first that by the energy conservation law, the work  $\mathcal{W}$  is given by the heat  $Q$  and the energy difference  $\Delta E$ , namely by  $\mathcal{W} = Q + \Delta E$ , where the energy difference  $\Delta E$  is the sum of the kinetic energy difference  $\Delta K$  and the potential energy difference  $\Delta U$ , i.e.  $\Delta E = \Delta U + \Delta K$ . Here, the kinetic energy difference  $\Delta K = \Delta K_c$  and  $\Delta K_l$  in the comoving frame and the laboratory frame are given by  $(m\dot{y}_t^2/2) - (m\dot{y}_{t_0}^2/2)$  and  $(m\dot{x}_t^2/2) - (m\dot{x}_{t_0}^2/2)$ , respectively, so that we obtain the relation

$$\Delta K_c = \Delta K_l - \int_{t_0}^t ds m\ddot{x}_s v. \quad (7)$$

Equation (7) means that the kinetic energy difference  $\Delta K$  depends on the frames and its frame-difference is determined by the d'Alembert-like force  $-m\ddot{x}_s$  as a purely inertial effect. This frame-difference of  $\Delta K$  also appears in the work, and leads to the relation  $\mathcal{W}_c = \mathcal{W}_l - \int_{t_0}^t ds m\ddot{x}_s v$ . A more complete explanation for this frame-dependence of the work is given in Ref. [6], based on a nonequilibrium generalization of the detailed balance condition.

To discuss these two different kinds of work done in the laboratory and comoving frames simultaneously in this paper, we consider the work defined in general by

$$\mathcal{W}(\{x_s\}) = \int_{t_0}^t ds [-\kappa(x_s - vs) - (1 - \vartheta)m\ddot{x}_s]v, \quad (8)$$

which gives the work  $\mathcal{W}_l$  done in the laboratory case ( $\vartheta = 1$ ) as well as the work  $\mathcal{W}_c$  done in the comoving case ( $\vartheta = 0$ ) by changing value of the parameter  $\vartheta$ . [25]

Using the functional average defined by Eq. (6), the probability distribution  $P_w(W)$  for the dimensionless work  $\beta\mathcal{W}(\{x_s\})$  is given by

$$P_w(W, t) = \langle\langle \delta(W - \beta\mathcal{W}(\{x_s\})) \rangle\rangle_t. \quad (9)$$

For later calculative convenience, we introduce a Fourier transformation  $\mathcal{E}_w(i\lambda, t)$  of the work distribution function  $P_w(W, t)$  through the function  $\mathcal{E}_w(\lambda, t)$  defined by

$$\mathcal{E}_w(\lambda, t) \equiv \langle\langle e^{-\lambda\beta\mathcal{W}(\{x_s\})} \rangle\rangle_t, \quad (10)$$

so that the work distribution function  $P_w(W)$  can be represented as

$$P_w(W, t) = \frac{1}{2\pi} \int_{-\infty}^{+\infty} d\lambda \mathcal{E}_w(i\lambda, t) e^{i\lambda W}. \quad (11)$$

The function  $\mathcal{E}_w(\lambda, t)$  can be also regarded as a generating function for the work  $\mathcal{W}(\{x_s\})$ . By Eq. (10) we obtain a useful identity

$$\mathcal{E}_w(0, t) = 1 \quad (12)$$

used to determine a normalization constant later [Eq. (43)].

## B. Path Integral Analysis for Work Distribution

To calculate the function  $\mathcal{E}_w(\lambda, t)$  from Eq. (10), we first note that

$$\begin{aligned} \mathcal{E}_w(\lambda, t) &= C_x \int \int dx_i dp_i \int_{(x_{t_0}, \dot{x}_{t_0})=(x_i, p_i/m)}^{(x_t, \dot{x}_t)=(x_f, p_f/m)} \mathcal{D}x_s \\ &\quad \times \int \int dx_f dp_f f(x_i, p_i, t_0) \\ &\quad \times \exp \left[ \int_{t_0}^t ds L(\ddot{x}_s, \dot{x}_s, x_s, s) \right] \end{aligned} \quad (13)$$

by Eqs. (5), (6), (8) and (10). Here,  $L(\ddot{x}_s, \dot{x}_s, x_s, s)$  is defined by

$$\begin{aligned} L(\ddot{x}_s, \dot{x}_s, x_s, s) &\equiv -\frac{1}{4D} \left( \dot{x}_s + \frac{x_s - vs}{\tau_r} + \frac{m}{\alpha} \ddot{x}_s \right)^2 \\ &\quad + \lambda \beta [\kappa(x_s - vs) + (1 - \vartheta)m\ddot{x}_s]v, \end{aligned} \quad (14)$$

which may be interpreted as a Lagrangian function including a Lagrange multiplier  $\lambda$  due to the restriction of the delta function for work in Eq. (9) [6][26]. Here, as elsewhere in this paper, the dependence of  $L(\ddot{x}_s, \dot{x}_s, x_s, s)$  on the parameters  $v$ ,  $\vartheta$ , etc., has not been explicitly indicated on the left-hand side of Eq. (14).

The first step to calculate the function  $\mathcal{E}_w(\lambda, t)$  is to specify the most-contributing path  $\{x_s^*\}_{s \in [t_0, t]}$  in the path integral involved on the right-hand side of Eq. (13). Such a special path  $\{x_s^*\}_{s \in [t_0, t]}$  is introduced as the one satisfying the variational principle

$$\delta \int_{t_0}^t ds L(\ddot{x}_s^*, \dot{x}_s^*, x_s^*, s) = 0 \quad (15)$$

with the four boundary conditions  $x_{t_0}^* = x_i$ ,  $\dot{x}_{t_0}^* = p_i/m$ ,  $x_t^* = x_f$  and  $\dot{x}_t^* = p_f/m$ . In a way similar to derive the Euler-Lagrange equation from the minimum action principle in analytical mechanics [19], Eq. (15) leads to

$$\begin{aligned} \frac{d^2}{ds^2} \frac{\partial L(\ddot{x}_s^*, \dot{x}_s^*, x_s^*, s)}{\partial \ddot{x}_s^*} - \frac{d}{ds} \frac{\partial L(\ddot{x}_s^*, \dot{x}_s^*, x_s^*, s)}{\partial \dot{x}_s^*} \\ + \frac{\partial L(\ddot{x}_s^*, \dot{x}_s^*, x_s^*, s)}{\partial x_s^*} = 0 \end{aligned} \quad (16)$$

for the Lagrangian function (14). Inserting Eq. (14) into Eq. (16) we obtain a fourth-order linear differential equation

$$\tau_m^2 \frac{d^4 \tilde{x}_s^*}{ds^4} - \left( 1 - 2\frac{\tau_m}{\tau_r} \right) \frac{d^2 \tilde{x}_s^*}{ds^2} + \frac{1}{\tau_r^2} \tilde{x}_s^* = 0 \quad (17)$$

for the function  $\tilde{x}_s^*$  of  $s$ , which is defined by

$$\tilde{x}_s^* \equiv x_s^* - vs + (1 - 2\lambda)v\tau_r, \quad (18)$$

using the inertial characteristic time  $\tau_m \equiv m/\alpha$ .

We consider solutions of Eq. (17) of the form  $\exp(\nu s)$ . Inserting  $\tilde{x}_s^* = \exp(\nu s)$  into Eq. (17) we obtain the quadratic equation

$$\begin{aligned} \tau_m^2 \nu^4 - \left(1 - 2\frac{\tau_m}{\tau_r}\right) \nu^2 + \frac{1}{\tau_r^2} \\ = \left(\tau_m \nu^2 + \nu + \frac{1}{\tau_r}\right) \left(\tau_m \nu^2 - \nu + \frac{1}{\tau_r}\right) \\ = 0 \end{aligned} \quad (19)$$

for  $\nu$ . The solutions of Eq. (19) are  $\nu = \nu_+, \nu_-, -\nu_-, -\nu_+$  using  $\nu_\pm$  defined by

$$\nu_\pm = \frac{1}{2\tau_m} \left(1 \pm \sqrt{1 - 4\frac{\tau_m}{\tau_r}}\right). \quad (20)$$

The general solution of the fourth-order differential equation (17) is represented as a superposition of these special solutions  $\exp(\nu s)$ ,  $\nu = \nu_+, \nu_-, -\nu_-, -\nu_+$ , namely

$$\tilde{x}_s^* = C_1 e^{\nu_+ s} + C_2 e^{\nu_- s} + C_3 e^{-\nu_- s} + C_4 e^{-\nu_+ s} \quad (21)$$

with constants  $C_j$ ,  $j = 1, 2, 3, 4$ . Using Eqs. (18) and (21) and introducing the four dimensional vector  $\mathbf{C} \equiv (C_1 \ C_2 \ C_3 \ C_4)^T$ , [27] we can rewrite

$$x_s^* = \mathbf{C}^T \mathbf{K}_s + v s - (1 - 2\lambda) v \tau_r \quad (22)$$

where the vector  $\mathbf{K}_s$  is defined by

$$\mathbf{K}_s \equiv \begin{pmatrix} e^{\nu_+ s} \\ e^{\nu_- s} \\ e^{-\nu_- s} \\ e^{-\nu_+ s} \end{pmatrix}. \quad (23)$$

The constant vector  $\mathbf{C}$  is determined by the four boundary conditions for  $x_s^*$  and we obtain

$$\mathbf{C} = A_t^{-1} \mathbf{B}_{if}^{(1-2\lambda)} \quad (24)$$

where the matrix  $A_t$  is defined by

$$A_t \equiv \begin{pmatrix} e^{\nu_+ t_0} & e^{\nu_- t_0} & e^{-\nu_- t_0} & e^{-\nu_+ t_0} \\ \nu_+ e^{\nu_+ t_0} & \nu_- e^{\nu_- t_0} & -\nu_- e^{-\nu_- t_0} & -\nu_+ e^{-\nu_+ t_0} \\ e^{\nu_+ t} & e^{\nu_- t} & e^{-\nu_- t} & e^{-\nu_+ t} \\ \nu_+ e^{\nu_+ t} & \nu_- e^{\nu_- t} & -\nu_- e^{-\nu_- t} & -\nu_+ e^{-\nu_+ t} \end{pmatrix} \quad (25)$$

and the vector  $\mathbf{B}_{if}^{(z)}$  is defined by

$$\mathbf{B}_{if}^{(z)} \equiv \begin{pmatrix} x_i - v t_0 \\ p_i/m - v \\ x_f - v t \\ p_f/m - v \end{pmatrix} + z v \tau_r \begin{pmatrix} 1 \\ 0 \\ 1 \\ 0 \end{pmatrix}. \quad (26)$$

It may be noted that the first component  $x_i - v t_0$  and the second component  $(p_i/m) - v$  (the third component  $x_f - v t_0$  and the fourth component  $(p_f/m) - v$ ) of the

vector  $\mathbf{B}_{if}^{(0)}$  can be regarded as the initial (final) position and velocity of the particle in the comoving frame, respectively.

As the next step, we represent a path  $\{x_s\}_{s \in [t_0, t]}$  as the sum of the most contributing path  $\{x_s^*\}_{s \in [t_0, t]}$  given by Eq. (22) and its deviation  $\{\Delta x_s\}_{s \in [t_0, t]}$  defined by

$$\Delta x_s \equiv x_s - x_s^*, \quad (27)$$

where the variable  $\Delta x_s$  satisfies the four boundary conditions  $\Delta x_{t_0} = \Delta x_t = 0$  and  $\dot{\Delta x}_{t_0} = \dot{\Delta x}_t = 0$  with  $\dot{\Delta x}_s \equiv d\Delta x_s/ds$ . Using this variable  $\Delta x_s$ , the complete time integral  $\int_{t_0}^t ds \ L(\ddot{x}_s, \dot{x}_s, x_s, s)$  of the Lagrangian function can be represented as

$$\begin{aligned} \int_{t_0}^t ds \ L(\ddot{x}_s, \dot{x}_s, x_s, s) \\ = \int_{t_0}^t ds \ L(\ddot{x}_s^*, \dot{x}_s^*, x_s^*, s) \\ - \frac{1}{4D} \int_{t_0}^t ds \ \left( \Delta \dot{x}_s + \frac{1}{\tau_r} \Delta x_s + \frac{m}{\alpha} \Delta \ddot{x}_s \right)^2 \end{aligned} \quad (28)$$

in terms of the two variables  $x_s^*$  and  $\Delta x_s$ . Inserting Eq. (28) into Eq. (13) we obtain

$$\begin{aligned} \mathcal{E}_w(\lambda, t) = C_{\mathcal{E}} \int \int dx_i dp_i \int \int dx_f dp_f \\ \times f(x_i, p_i, t_0) \exp \left[ \int_{t_0}^t ds \ L(\ddot{x}_s^*, \dot{x}_s^*, x_s^*, s) \right] \end{aligned} \quad (29)$$

where  $C_{\mathcal{E}}$  is defined by  $C_{\mathcal{E}} \equiv C_x \int_{(\Delta x_{t_0}, \Delta \dot{x}_{t_0})=(0,0)}^{(\Delta x_t, \Delta \dot{x}_t)=(0,0)} \mathcal{D} \Delta x_s \exp[-(1/4D) \int_{t_0}^t ds \ \int_{t_0}^t ds \ (\Delta \dot{x}_s + (1/\tau_r) \Delta x_s + (m/\alpha) \Delta \ddot{x}_s)^2]$  and is independent of  $\lambda$ . In the expression (29), the contributions of the deviations  $\Delta x_s$  to the path integral in the function  $\mathcal{E}_w(\lambda, t)$  are included only in the coefficient  $C_{\mathcal{E}}$ .

Next, we calculate the quantity  $\int_{t_0}^t ds \ L(\ddot{x}_s^*, \dot{x}_s^*, x_s^*, s)$  using Eq. (22), and then the function  $\mathcal{E}_w(\lambda, t)$  given by Eq. (29). For such a calculation, using Eq. (22) we first note that

$$\frac{dx_s^*}{ds} = \mathbf{C}^T \Theta \mathbf{K}_s + v, \quad (30)$$

$$\frac{d^2 x_s^*}{ds^2} = \mathbf{C}^T \Theta^2 \mathbf{K}_s \quad (31)$$

where the  $4 \times 4$  matrix  $\Theta$  is defined by

$$\Theta \equiv \begin{pmatrix} \nu_+ & 0 & 0 & 0 \\ 0 & \nu_- & 0 & 0 \\ 0 & 0 & -\nu_- & 0 \\ 0 & 0 & 0 & -\nu_+ \end{pmatrix}. \quad (32)$$

Then, using Eqs. (22), (30) and (31) we obtain

$$\dot{x}_s^* + \frac{x_s^* - v s}{\tau_r} + \frac{m}{\alpha} \ddot{x}_s^* = \mathbf{C}^T \Gamma \mathbf{K}_s + 2\lambda v \quad (33)$$

where the matrix  $\Gamma$  is introduced as

$$\begin{aligned}\Gamma &\equiv \tau_m \Theta^2 + \Theta + \frac{1}{\tau_r} \mathcal{I} \\ &= 2 \begin{pmatrix} \nu_+ & 0 & 0 & 0 \\ 0 & \nu_- & 0 & 0 \\ 0 & 0 & 0 & 0 \\ 0 & 0 & 0 & 0 \end{pmatrix}\end{aligned}\quad (34)$$

with the relation  $\tau_m \nu_{\pm}^2 - \nu_{\pm} + \tau_r^{-1} = 0$  and  $\mathcal{I}$  the  $4 \times 4$  identity matrix. Using Eqs. (14), (22), (31) and (33) we obtain

$$\begin{aligned}L(\ddot{x}_s^*, \dot{x}_s^*, x_s^*, s) &= -\frac{1}{4} \alpha \beta \mathbf{C}^T \Gamma \mathbf{K}_s \mathbf{K}_s^T \Gamma \mathbf{C} \\ &\quad - \alpha \beta \lambda v \mathbf{C}^T [\tau_m \vartheta \Theta^2 + \Theta] \mathbf{K}_s \\ &\quad - \lambda(1 - \lambda) \alpha \beta v^2.\end{aligned}\quad (35)$$

Noting Eq. (24) and that

$$\begin{aligned}\int_{t_0}^t ds \mathbf{C}^T \Theta \mathbf{K}_s &= \int_{t_0}^t ds \frac{dx_s^*}{ds} - v(t - t_0) \\ &= x_f - x_i - v(t - t_0),\end{aligned}\quad (36)$$

$$\int_{t_0}^t ds \mathbf{C}^T \Theta^2 \mathbf{K}_s = \int_{t_0}^t ds \frac{d^2 x_s^*}{ds^2} = \frac{p_f - p_i}{m} \quad (37)$$

by Eqs. (30) and (31), we further obtain

$$\begin{aligned}\int_{t_0}^t ds L(\ddot{x}_s^*, \dot{x}_s^*, x_s^*, s) &= -\frac{1}{4} \alpha \beta [\mathbf{B}_{if}^{(1-2\lambda)}]^T \Lambda_t \mathbf{B}_{if}^{(1-2\lambda)} - \alpha \beta \lambda v \boldsymbol{\eta}^T \mathbf{B}_{if}^{(0)} \\ &\quad - \lambda(1 - \lambda) \alpha \beta v^2 (t - t_0)\end{aligned}\quad (38)$$

where the  $4 \times 4$  matrix  $\Lambda_t$  and the vector  $\boldsymbol{\eta}$  are defined by

$$\Lambda_t \equiv (A_t^{-1})^T \Gamma \Phi_t \Gamma A_t^{-1}, \quad (39)$$

$$\boldsymbol{\eta} \equiv \begin{pmatrix} -1 \\ -\tau_m \vartheta \\ 1 \\ \tau_m \vartheta \end{pmatrix}, \quad (40)$$

respectively, with the  $4 \times 4$  matrix  $\Phi_t$  defined by

$$\Phi_t \equiv \int_{t_0}^t ds \mathbf{K}_s \mathbf{K}_s^T. \quad (41)$$

Inserting Eq. (38) into Eq. (29) we obtain

$$\begin{aligned}\mathcal{E}_w(\lambda, t) &= C_{\mathcal{E}} e^{-\lambda(1-\lambda)\alpha\beta v^2(t-t_0)} \int \int dx_i dp_i \int \int dx_f dp_f f(x_i, p_i, t_0) \\ &\quad \times \exp \left\{ -\frac{1}{4} \alpha \beta [\mathbf{B}_{if}^{(1-2\lambda)}]^T \Lambda_t \mathbf{B}_{if}^{(1-2\lambda)} - \alpha \beta \lambda v \boldsymbol{\eta}^T \mathbf{B}_{if}^{(0)} \right\}.\end{aligned}\quad (42)$$

Equation (42) gives a concrete form of the function  $\mathcal{E}_w(\lambda, t)$  for any initial distribution function  $f(x_i, p_i, t_0)$ .

The  $\lambda$ -independent normalization coefficient  $C_{\mathcal{E}}$  in Eq. (42) can be determined from the condition (12), and we obtain

$$C_{\mathcal{E}} = \left\{ \int \int dx_i dp_i \int \int dx_f dp_f f(x_i, p_i, t_0) \exp \left\{ -\frac{1}{4} \alpha \beta [\mathbf{B}_{if}^{(1)}]^T \Lambda_t \mathbf{B}_{if}^{(1)} \right\} \right\}^{-1}. \quad (43)$$

Note that by using the condition (12) we avoided to carry out explicitly the path integral included originally in the quantity  $C_{\mathcal{E}}$  [cf. Eq. (29)].

Inserting Eq. (42) into Eq. (11), and carrying out the Gaussian integral over  $\lambda$  appearing then in Eq. (11), we obtain

$$\begin{aligned}P_w(W, t) &= \frac{C_{\mathcal{E}}}{\sqrt{4\pi\alpha\beta v^2(t-t_0 - \tau_r^2 \mathbf{J}^T \Lambda_t \mathbf{J})}} \int \int dx_i dp_i \int \int dx_f dp_f f(x_i, p_i, t_0) \\ &\quad \times \exp \left\{ -\frac{1}{4} \alpha \beta [\mathbf{B}_{if}^{(1)}]^T \Lambda_t \mathbf{B}_{if}^{(1)} - \frac{\left\{ W - \alpha \beta v [v(t-t_0) + (\boldsymbol{\eta}^T - \tau_r \mathbf{J}^T \Lambda_t) \mathbf{B}_{if}^{(1)}] \right\}^2}{4\alpha\beta v^2(t-t_0 - \tau_r^2 \mathbf{J}^T \Lambda_t \mathbf{J})} \right\}\end{aligned}\quad (44)$$

where the 4-dimensional vector  $\mathbf{J}$  is defined by

$$\mathbf{J} \equiv \begin{pmatrix} 1 \\ 0 \\ 1 \\ 0 \end{pmatrix} \quad (45)$$

and we used the relation  $\boldsymbol{\eta}^T \mathbf{J} = 0$ . Equation (44) is an explicit form for the work distribution function for all

time, and for any initial distribution function  $f(x_i, p_i, t_0)$ . Using Eq. (43) for the coefficient  $C_\varepsilon$ , the work distribution function (44) is properly normalized, namely  $\int dW P_w(W, t) = 1$ , at any time  $t$ .

In the next two sections IV and V we discuss, using the work distribution function (44), fluctuation properties of the work from the viewpoint of the asymptotic fluctuation theorem for  $t \rightarrow +\infty$ , as well as for finite times.

#### IV. ASYMPTOTIC FLUCTUATION THEOREM

The matrix  $\Lambda_t$  defined by Eq. (39) satisfies the condition

$$\lim_{t \rightarrow +\infty} \frac{1}{t - t_0} \Lambda_t = 0, \quad (46)$$

as shown in Appendix A. Equation (46) implies that  $v(t - t_0) + (\boldsymbol{\eta}^T - \tau_r \mathbf{J}^T \Lambda_t) \mathbf{B}_{if}^{(1)} \stackrel{t \rightarrow +\infty}{\sim} v(t - t_0)$  and  $t - t_0 - \tau_r^2 \mathbf{J}^T \Lambda_t \mathbf{J} \stackrel{t \rightarrow +\infty}{\sim} t - t_0$  in Eq. (44), so that the work distribution function  $P_w(W, t)$  is proportional to the Gaussian function  $\exp\{-[W - \alpha\beta v^2(t - t_0)]^2 / [4\alpha\beta v^2(t - t_0)]\}$  in the long time limit  $t \rightarrow +\infty$ , i.e.

$$P_w(W, t) \stackrel{t \rightarrow +\infty}{\sim} \frac{1}{\sqrt{4\pi\alpha\beta v^2(t - t_0)}} \times \exp\left\{-\frac{[W - \alpha\beta v^2(t - t_0)]^2}{4\alpha\beta v^2(t - t_0)}\right\} \quad (47)$$

regardless of the initial distribution function  $f(x_i, p_i, t_0)$ . It is important to note that the work distribution function (47) in the long time limit  $t \rightarrow +\infty$  in the inertial case is the same as in the over-damped case. Physically, this is, of course, due to the finiteness of the inertial characteristic time  $\tau_m$ , which makes inertial effects disappear in the long time limit. Nevertheless, the proof of this equivalence is non-trivial.

From Eq. (47) we immediately derive

$$\lim_{t \rightarrow +\infty} \frac{P_w(W, t)}{P_w(-W, t)} = e^W \quad (48)$$

for any initial distribution function  $f(x_i, p_i, t_0)$ . We will call Eq. (48) the asymptotic fluctuation theorem for work. Equation (48) is independent of the value of the parameter  $\vartheta$ , i.e. of the frame of reference (laboratory or comoving) or also of the contribution of the d'Alembert-like force to the work (8).

#### V. INERTIAL EFFECTS FOR FINITE TIMES

##### A. Slope of $\ln[P_w(W, t)/P_w(-W, t)]$ and the Critical Mass

In contrast to the asymptotic work distribution function (47), various inertial effects in the work distribution function appear for finite times. In this section we discuss such inertial effects using the function  $G(W, t)$  defined by

$$G(W, t) \equiv \frac{\partial}{\partial W} \ln \frac{P_w(W, t)}{P_w(-W, t)}. \quad (49)$$

The function  $G(W, t)$  gives the slope of the fluctuation function  $\ln[P_w(W, t)/P_w(-W, t)]$  with respect to  $W$ , and satisfies

$$\lim_{t \rightarrow +\infty} G(W, t) = 1 \quad (50)$$

by the asymptotic fluctuation theorem (48).[28]

The behavior of  $G(W, t)$  for finite times depends on the initial condition. To get concrete results, in this section we concentrate on the case of a nonequilibrium steady state initial condition, which can be represented by

$$f(x_i, p_i, t_0) = \frac{\beta}{2\pi} \sqrt{\frac{\kappa}{m}} \exp\left\{-\beta \left[\frac{(p_i - mv)^2}{2m} + \frac{1}{2}\kappa(x_i - vt_0 + v\tau_r)^2\right]\right\} \quad (51)$$

for any frame. The initial distribution function (51) gives a Gaussian distribution for the particle initial position  $x_i$  and momentum  $p_i$  around their nonequilibrium steady state average values  $vt_0 - v\tau_r$  and  $mv$ , respectively. Inserting Eq. (51) into Eq. (44) the work distribution function is given by

$$P_w(W, t) = \sqrt{\frac{1 - \Omega_t}{4\pi\alpha\beta v^2(t - t_0 - \tau_r^2 \mathbf{J}^T \Lambda_t \mathbf{J})}} \exp\left\{-\frac{1 - \Omega_t}{4\alpha\beta v^2(t - t_0 - \tau_r^2 \mathbf{J}^T \Lambda_t \mathbf{J})} [W - \alpha\beta v^2(t - t_0)]^2\right\} \quad (52)$$

where  $\Omega_t$  is defined by

$$\Omega_t \equiv (\boldsymbol{\eta} - \tau_r \Lambda_t \mathbf{J})^T \left[ (\boldsymbol{\eta} - \tau_r \Lambda_t \mathbf{J}) (\boldsymbol{\eta} - \tau_r \Lambda_t \mathbf{J})^T + (t - t_0 - \tau_r^2 \mathbf{J}^T \Lambda_t \mathbf{J}) (\Lambda^{(0)} + \Lambda_t) \right]^{-1} (\boldsymbol{\eta} - \tau_r \Lambda_t \mathbf{J}). \quad (53)$$

with the  $4 \times 4$  matrix  $\Lambda^{(0)}$  defined by

$$\Lambda^{(0)} \equiv \frac{2}{\alpha} \begin{pmatrix} \kappa & 0 & 0 & 0 \\ 0 & m & 0 & 0 \\ 0 & 0 & 0 & 0 \\ 0 & 0 & 0 & 0 \end{pmatrix}. \quad (54)$$

[See Appendix B for a derivation of Eq. (52).] Note that

the work distribution function (52) is Gaussian with the average work  $\langle W \rangle = \alpha\beta v^2(t - t_0)$  at any time because we chose a Gaussian nonequilibrium steady state initial condition (51). Since the work distribution function  $P(W, t)$  is Gaussian,  $G(W, t)$  defined by Eq. (49) is independent of  $W$ , so that we denote it by  $G(t) [= G(W, t)]$  from now on. Inserting Eq. (52) into Eq. (49), we obtain

$$G(t) = \frac{1 - \Omega_t}{1 - \frac{\tau_r^2}{t - t_0} \mathbf{J}^T \Lambda_t \mathbf{J}} \quad (55)$$

as an explicit form of  $G(t)$ . One may notice that  $G(t)$  in Eq. (55) is independent of the dragging velocity  $v$  and the inverse temperature  $\beta$ . Moreover,  $G(t)$  is positive for  $t > t_0$  because the distribution function  $P_w(W, t)$  is normalizable so that the coefficient  $(1 - \Omega_t)/[4\alpha\beta v^2(t - t_0 - \tau_r^2 \mathbf{J}^T \Lambda_t \mathbf{J})] = G(t)/[4\alpha\beta v^2(t - t_0)]$  in the exponent of the Gaussian distribution function (52) must be positive.

As a first approximation to the asymptotic relaxation of  $G(t)$  to its final value (50), we obtain from Eq. (55)

$$G(t) \stackrel{t \rightarrow +\infty}{\sim} 1 + \frac{\tau_r - \tau_m \vartheta^2}{t - t_0 - \tau_r + \tau_m \vartheta^2}, \quad (56)$$

meaning that the function  $G(t)$  decays to 1 by a power inversely proportional to the time in the long time limit  $t \rightarrow +\infty$ . [See Appendix C for a derivation of Eq. (56).] Equation (56) is only the first approximation for an asymptotic form of  $G(t)$ , but already includes an important inertial contribution to  $G(t)$ , as well as an interesting frame dependence of  $G(t)$ . Actually, the second term on the right-hand side of Eq. (56) depends on the mass  $m$  via  $\tau_m = m/\alpha$  in the laboratory frame  $\vartheta = 1$ , while that term is independent of the mass in the comoving frame  $\vartheta = 0$ . Another interesting property of  $G(t)$  expressed by Eq. (56) is that in the laboratory frame  $\vartheta = 1$  the second term on the right-hand side of Eq. (56), the  $t^{-1}$ -decay term of  $G(t)$ , vanishes in the case that  $\tau_r = \tau_m$ , i.e. for a special mass value  $m = \alpha^2/\kappa$ .

Perhaps the most interesting implication of Eq. (55) for  $G(t)$ , although it does not appear explicitly in the asymptotic expression (56) of  $G(t)$ , is the existence of a critical value of the mass  $m = m^*$  above which  $G(t)$  shows a time-oscillatory behavior. In our theory, this time-oscillation has its origin in the time-dependence of  $\tilde{x}_s^*$  given by Eq. (21) via the exponential terms  $\exp(\nu_\pm t)$ , etc., when the coefficient  $\nu_\pm$  given by Eq. (20) has an imaginary part, namely when the condition

$$m > m^* \equiv \frac{\alpha^2}{4\kappa} \quad (57)$$

(derived from the condition  $4\tau_m\tau_r^{-1} - 1 > 0$ ) is satisfied. We call the mass  $m^*$  the critical mass in this paper, since a (smooth) “dynamical” phase transition takes place at  $m = m^*$ . For masses  $m > m^*$ , the position  $\tilde{x}_s^*$  has a time-oscillation with the oscillation period  $\mathcal{T}_m$

$$\mathcal{T}_m = 2\pi\sqrt{\frac{m}{\kappa}} \left(1 - \frac{m^*}{m}\right)^{-1/2} \quad (58)$$

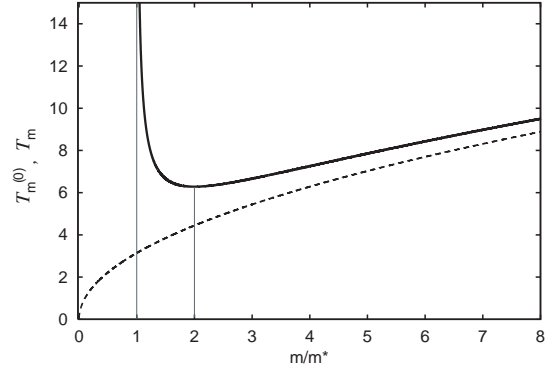


FIG. 1: Time oscillation period  $\mathcal{T}_m$  (solid line) in  $\tilde{x}_s^*$  as a function of mass  $m$  normalized by the critical mass  $m^* \equiv \alpha^2/(4\kappa)$  for the mass in  $m/m^* > 1$ . There is no time-oscillation for  $m/m^* < 1$  and the minimum of  $\mathcal{T}_m$  is at  $m/m^* = 2$ . Here, we used parameter values  $\alpha = \kappa = 1$ . We also plotted a time-oscillation period  $\mathcal{T}_m^{(0)} = \mathcal{T}_m|_{\alpha=0} (= 2\pi\sqrt{m/\kappa})$  (broken line) for a purely harmonic oscillation in the case without the dissipation ( $\alpha = 0$ ). The time-oscillation period  $\mathcal{T}_m$  approaches  $\mathcal{T}_m^{(0)}$  in the large mass limit  $m/m^* \rightarrow +\infty$ .

corresponding to a frequency  $\omega \equiv \sqrt{4\tau_m\tau_r^{-1} - 1}/(2\tau_m) = |Im\{\nu_\pm\}|$ , using the imaginary part  $Im\{\nu_\pm\}$  of  $\nu_\pm$ . In Fig. 1 the time-oscillation period  $\mathcal{T}_m$  (solid line) is shown as a function of the scaled mass  $m/m^*$  for  $m/m^* > 1$ . There is no time-oscillation of  $\tilde{x}_s^*$  in the case of  $m/m^* < 1$ , and the time-oscillation period diverges when  $m/m^* \rightarrow 1 + 0$ . The oscillation period  $\mathcal{T}_m$  decreases rapidly as a function of mass  $m$  for  $m/m^* < 2$ , has a minimum at  $m/m^* = 2$ , and increases gradually for  $m/m^* > 2$ . For comparison, we also plotted in Fig. 1 the scaled mass dependence of the time-oscillation period  $\mathcal{T}_m^{(0)} = 2\pi\sqrt{m/\kappa} (= \mathcal{T}_m|_{\alpha=0})$  (broken line) for a purely harmonic oscillator with spring constant  $\kappa$ . Different from the time-oscillation period (58), the period  $\mathcal{T}_m^{(0)}$  is defined for all the masses, and increases monotonically as the mass increases. The time-oscillation period (58) approaches  $\mathcal{T}_m^{(0)}$  in the large mass limit  $m/m^* \rightarrow +\infty$ .

It is useful to consider the critical behavior in the time-oscillating behavior of  $G(t)$  as due to the presence of *two* independent time scales appearing in our model: one characterized by  $\tau_r (= \alpha/\kappa)$  and another by  $\tau_m (= m/\alpha)$ . These time scales  $\tau_m$  and  $\tau_r$  are related by  $\tau_r = 4\tau_m^*$  at the critical mass  $m = m^*$ . Using these two time scales, the time oscillation period  $\mathcal{T}_m^{(0)}$  for a purely harmonic oscillator is given by  $\mathcal{T}_m^{(0)} = 2\pi\sqrt{\tau_r\tau_m}$ . Introducing the frequencies  $\omega^{(0)} \equiv 2\pi/\mathcal{T}_m^{(0)}$  and  $\omega_m \equiv 1/\tau_m$  corresponding to the two time scales  $\mathcal{T}_m^{(0)}$  and  $\tau_m$ , respectively, the frequency  $\omega \equiv 2\pi/\mathcal{T}_m$  is represented as  $\omega = \sqrt{[\omega^{(0)}]^2 - \omega_m^2/4}$  corresponding to the time-oscillation period (58). In this expression for the fre-

quency  $\omega$  the time oscillations occur only when the condition  $[\omega^{(0)}]^2 > \omega_m^2/4$  is satisfied. The existence of these two time scale  $\tau_m$  and  $\tau_r$  is therefore essential for the time-oscillatory behavior with the frequency  $\omega$ , noting that there is no time-oscillation in the over-damped case containing only  $\tau_r$ .

In the next two subsections VB and VC, we investigate properties of  $G(t)$  in more detail, including its time-oscillating behavior, for (A) the work done in the laboratory frame ( $\vartheta = 1$ ), and (B) the work done in the comoving frame ( $\vartheta = 0$ ), separately. We will also compare those results with those for the over-damped case. For this purpose, we now calculate  $G(t)$  explicitly in the over-damped case. In our previous paper [6], we already calculated the work distribution function  $P_w^{(0)}(W, t)$  for the over-damped case, which is given by

$$P_w^{(0)}(W, t) = \frac{1}{\sqrt{4\pi\alpha\beta v^2 [t - t_0 - \tau_r(1 - b_t)]}} \times \exp \left\{ -\frac{[W - \alpha\beta v^2(t - t_0)]^2}{4\alpha\beta v^2 [t - t_0 - \tau_r(1 - b_t)]} \right\} \quad (59)$$

with  $b_t \equiv \exp[-(t - t_0)/\tau_r]$  in the case of a nonequilibrium steady state initial distribution function  $f^{(0)}(x_i, t_0) = \sqrt{\beta\kappa/(2\pi)} \exp[-\beta\kappa(x_i - vt_0 + v\tau_r)^2/2]$  for the particle position  $x_i$  for the over-damped case at the initial time  $t_0$ . [29] Using Eq. (59), and defining, [cf. Eq. (49)],  $G^{(0)}(t) \equiv (\partial/\partial W) \ln[P_w^{(0)}(W, t)/P_w^{(0)}(-W, t)]$ , we have

$$G^{(0)}(t) = 1 + \frac{\tau_r(1 - b_t)}{t - t_0 - \tau_r(1 - b_t)}, \quad (60)$$

which gives  $G(t)$  for the over-damped case [21]. Note that Eq. (60) implies  $G^{(0)}(t) \xrightarrow{t \rightarrow +\infty} 1 + \tau_r/(t - t_0 - \tau_r)$ , which is consistent with Eq. (56), since  $\tau_m$  is zero for the over-damped case.

### B. $G(t)$ in the Laboratory Frame

In this subsection we consider  $G(t)$  given by Eq. (55) – which depends on the parameter  $\vartheta$  to specify a frame via  $\Lambda_t$  and  $\Omega_t$  – for the work done in the laboratory frame, i.e. for  $\vartheta = 1$ . In this subsection VB, as well as in the next subsection VC, we use the parameter values  $\alpha = \kappa = 1$  and set the initial time  $t_0 = 0$ , i.e.  $\tau_r = 1$  as a time unit and  $m/m^* = 4\tau_m$  as the scaled mass.

Figure 2 shows  $G(t)$  given by Eq. (55) as a function of time  $t$  for the scaled masses  $m/m^* = 0$  (over-damped case), 0.999, 2, 4, 8, 20 and 40. The graphs of  $G(t)$  all converge to 1 in the long time limit  $t \rightarrow +\infty$ , as required by the asymptotic fluctuation theorem (48), i.e. by Eq. (50).

We now discuss in some detail the properties of Fig. 2. This figure shows that  $G(t)$  for nonzero masses is always smaller than in the over-damped case of zero mass. In

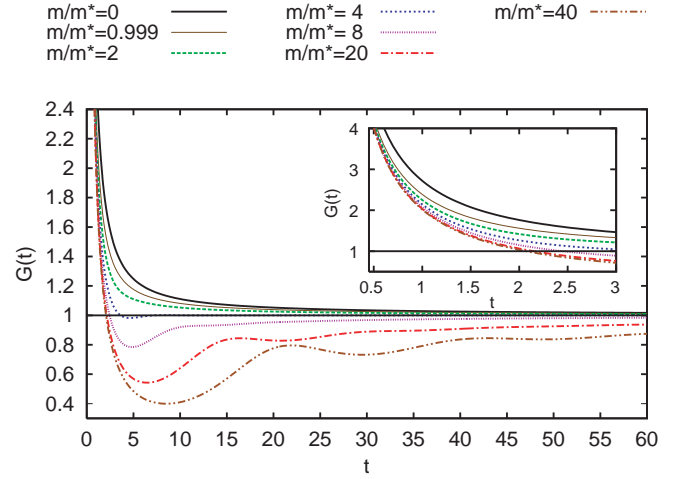


FIG. 2: (color online) Graphs of  $G(t) = (\partial/\partial W) \ln[P_w(W, t)/P_w(-W, t)]$  as a function of time  $t$  for the work done in the laboratory frame ( $\vartheta = 1$ ) in the case of a nonequilibrium steady state initial condition for  $t \in [0, 60]$ . Inset: Graphs of  $G(t)$  in a short time period for  $t \in [0, 3]$ . Lines in these graphs correspond to parameter values of the scaled masses  $m/m^* = 0$  (over-damped case), 0.999, 2, 4, 8, 20 and 40 as indicated above this figure, and we used parameter values  $\alpha = \kappa = 1$  (so that  $\tau_r = 1$  for a unit time and also  $m/m^* = 4\tau_m$  as the scaled mass, with  $m^* = 1/4$ ) and  $t_0 = 0$ .

the over-damped case,  $G(t)$  decreases monotonically to the final value 1 from  $+\infty$  at the initial time. A similar behavior is still observed for small masses (e.g. see the graph for  $m/m^* = 0.999$  in Fig. 2). It may also be noted that for small nonzero masses the relaxation of  $G(t)$  to its final value 1 is faster than in the over-damped case (e.g. see the graphs for  $m/m^* = 2$  and 4 in Fig. 2). This feature can be explained by the second term on the right-hand side of Eq. (56), since the absolute value  $|\tau_r - \tau_m|$  of the numerator of this term is smaller for  $\vartheta = 1$  than the corresponding over-damped value  $\tau_r$  in the case of  $0 < m/m^* < 8$ , using that  $|\tau_r - \tau_m| < \tau_r$ . Moreover, Fig. 2 shows that for large masses (e.g. see the graphs for  $m/m^* > 4$  in Fig. 2),  $G(t)$  is smaller than 1 for long times, while  $G(t)$  is always larger than 1 in the over-damped case. This is because the second term on the right-hand side of Eq. (56) is negative for  $\tau_r < \tau_m$  (i.e.  $m/m^* > 4$ ), when  $\vartheta = 1$  and  $t > t_0 + \tau_r - \tau_m$ .

A time-oscillatory behavior of  $G(t)$  is clearly visible in Fig. 2 for large masses, i.e. for  $m \gg m^*$ . To show more clearly the time-oscillatory behavior of  $G(t)$  for  $m > m^*$  as opposed to for  $m < m^*$ , we plotted in Fig. 3 the absolute value of the deviation [30]

$$\Delta G(t) \equiv G(t) - 1 - \frac{\tau_r - \tau_m \vartheta^2}{t - t_0 - \tau_r + \tau_m \vartheta^2} \quad (61)$$

of  $G(t)$  from its asymptotic form (56) as a function of



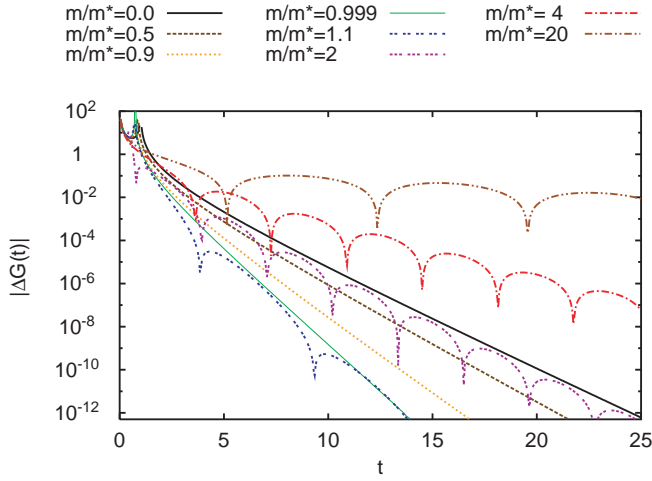


FIG. 3: (color online) Linear-log plots of absolute value  $|\Delta G(t)|$  of the function  $\Delta G(t) = G(t) - 1 - (\tau_r - \tau_m)/(t - \tau_r + \tau_m)$  as a function of time  $t$  for the work done in the laboratory frame in the case of a nonequilibrium steady state initial condition. Lines in these graphs correspond to parameter values of the scaled masses  $m/m^* = 0, 0.5, 0.9, 0.999, 1.1, 2, 4$  and  $20$  as indicated above this figure. The minima of the oscillations of  $|\Delta G(t)|$  for  $m/m^* > 1$  are actually zero, which is not indicated in this figure and Figs. 4, 6 and 7. We use the same parameter values  $\alpha, \kappa$  and  $t_0$  as in Fig. 2.

time  $t \in [0, 25]$  for the cases of  $m/m^* = 0, 0.5, 0.9, 0.999, 1.1, 2, 4$  and  $20$ . To illustrate the long time behavior of  $|\Delta G(t)|$  in more detail, we also show in Fig. 4 the absolute value  $|\Delta G(t)|$  of  $\Delta G(t)$  as functions of  $t \in [0, 1000]$  for the scaled masses  $m/m^* = 100, 200$  and  $1600$  as linear-log plots. The deviation  $\Delta G(t)$  goes to zero when  $t \rightarrow +\infty$  because of the asymptotic fluctuation theorem (50). In Figs. 3 and 4, it is important to note that there is no time-oscillation of  $\Delta G(t)$  for  $0 \leq m/m^* < 1$ , while we do observe time-oscillations of  $\Delta G(t)$  for  $m/m^* > 1$ , in agreement with a critical mass (57), above which  $G(t)$  oscillates in time. The decay of  $|\Delta G(t)|$  to zero as a function of  $t$  is faster for larger masses for  $0 \leq m/m^* < 1$  (cf. Fig. 3), but slower for larger masses for  $m/m^* > 1$  (cf. Figs. 3 and 4).

To check that the time oscillation period  $\mathcal{T}_m$  given by Eq. (58) indeed appears in  $G(t)$ , we fitted the data for  $\Delta G(t)$  to the function

$$\Delta G(t) \stackrel{t \rightarrow +\infty}{\sim} a e^{-bt} \sin\left(\frac{2\pi}{\mathcal{T}_m} t + c\right) \quad (62)$$

with fitting parameters  $a, b$  and  $c$  in Fig. 4. The values of the fitting parameters  $a, b$  and  $c$  are given in Table I. The function (62) is then sufficiently close to  $\Delta G(t)$  over many time-oscillation periods (except for short times), to suggest that the time-oscillations of  $G(t)$  may well have the same origin as those in the position  $\hat{x}_s^*$ . Similarly for

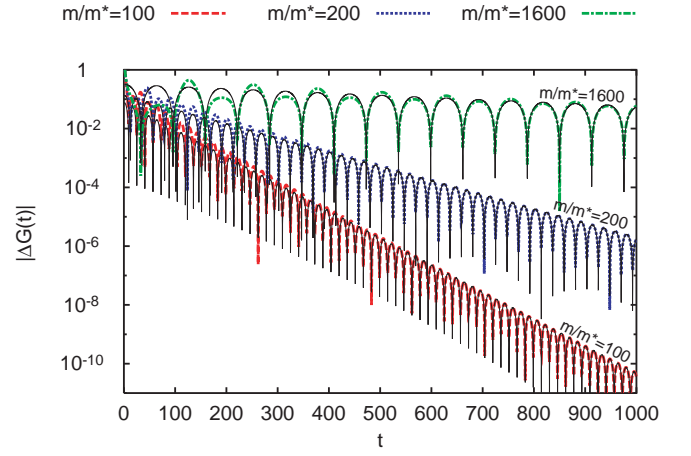


FIG. 4: (color online) Long time behavior of  $|\Delta G(t)|$  as a function of time  $t$  as linear-log plots for the work done in the laboratory frame in the case of a nonequilibrium steady state initial condition. Here, we use the same parameter values  $\alpha, \kappa$  and  $t_0$  as in Fig. 2. Broken, dotted and dash-dotted lines in these graphs correspond to parameter values of the scaled masses  $m/m^* = 100, 200$  and  $1600$ , respectively. Solid lines are fits of  $|\Delta G(t)|$  to the function (62) using Table I, together with the time-oscillation period (58), but they are visually indistinguishable from the graphs of  $|\Delta G(t)|$  except for short times.

Fig. 3, using the fitting function (62) we can also check that the time-oscillation periods of  $|\Delta G(t)|$  in this figure are given by Eq. (58). We fully realize that Figs. 3 and 4 are not enough to specify convincingly the function form of decay of  $\Delta G(t)$ . In Eq. (62) we assumed an exponential decay by a factor  $a \exp(-bt)$ , which seems to fit reasonably well the data in Fig. 4. However, values of the fitting parameters  $a$  and  $b$  shown in Table I appear to vary non-negligibly if we fit data including longer time periods than the ones shown in Fig. 4. In this sense, at this stage, the exponential factor in Eq. (62) should be regarded only as a convenience to check numerically the time oscillation period  $\mathcal{T}_m$  appearing in  $\Delta G(t)$ , rather than claiming an asymptotic exponential decay of  $\Delta G(t)$  of the form (62).

### C. $G(t)$ in the Comoving Frame

Here we consider  $G(t)$  for the work done in the comoving frame, namely the case of  $\vartheta = 0$ , in which the work includes effects of an inertial or d'Alembert-like force.

Figure 5 shows graphs of  $G(t)$  given by Eq. (55) as a function of time  $t$ . We chose the same masses as in Fig. 2, namely  $m/m^* = 0$  (over-damped case),  $0.999, 2, 4, 8, 20$  and  $40$  with the critical mass  $m^* = 1/4$ . It is clear that in Fig. 5 graphs of  $G(t)$  approach 1 as  $t \rightarrow +\infty$ , confirming the asymptotic fluctuation theorem (48).

Frame ( $\vartheta$ )	$m/m^*$	$\mathcal{T}_m$	a	b	c
Laboratory (1)	100	31.6	-0.077	0.021	4.4
Laboratory (1)	200	44.5	-0.14	0.011	4.5
Laboratory (1)	1600	125.7	-0.32	0.0017	4.6
Comoving (0)	100	31.6	0.0038	0.021	4.6
Comoving (0)	200	44.5	0.0035	0.011	4.6
Comoving (0)	1600	125.7	0.0032	0.0024	4.7

TABLE I: Values of the fitting parameters  $a$ ,  $b$  and  $c$  for the function (62) plotted in Figs. 3 and 6 for the parameter values  $\alpha = \kappa = 1$ .

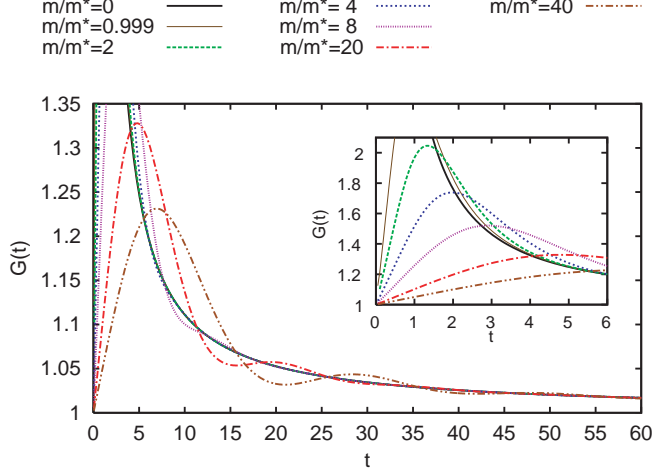


FIG. 5: (color online) Graphs of  $G(t) = (\partial/\partial W) \ln[P_w(W, t)/P_w(-W, t)]$  as a function of time  $t$  for the work done in the comoving frame ( $\vartheta = 0$ ) in the case of a nonequilibrium steady state initial condition for  $t \in [0, 60]$ . Inset: Graphs of  $G(t)$  in a short time period for  $t \in [0, 6]$ . Lines in these graphs correspond to parameter values of the scaled masses  $m/m^* = 0$  (over-damped case), 0.999, 2, 4, 8, 20 and 40 as indicated above this figure and we use the same parameter values  $\alpha$ ,  $\kappa$  and  $t_0$  as in Fig. 2.

Comparing Fig. 2 with Fig. 5, a dramatic difference in the behavior of  $G(t)$  in the two frames is clearly visible. First, a striking frame-dependence of  $G(t)$  is that for any nonzero mass,  $G(t)$  in the comoving frame starts from a finite value at the initial time  $t_0 (= 0)$  and is always larger than 1, in fact going through a maximum to its final value 1. This contrary to in the laboratory frame where  $G(t)$  diverges for  $t \rightarrow t_0 + 0$  and can be smaller than 1 for large masses and long times as discussed in Sec. VB. Another remarkable point is that, different from in the laboratory frame as shown in Fig. 2,  $G(t)$  converges to the over-damped line, much before converging to its final value 1, as shown in Fig. 5. This feature can be explained by the asymptotic form (56) of  $G(t)$ , whose right-hand side is independent of the mass  $m$  in the comoving frame ( $\vartheta = 0$ ), so a relaxation behavior of  $G(t)$  to its final value

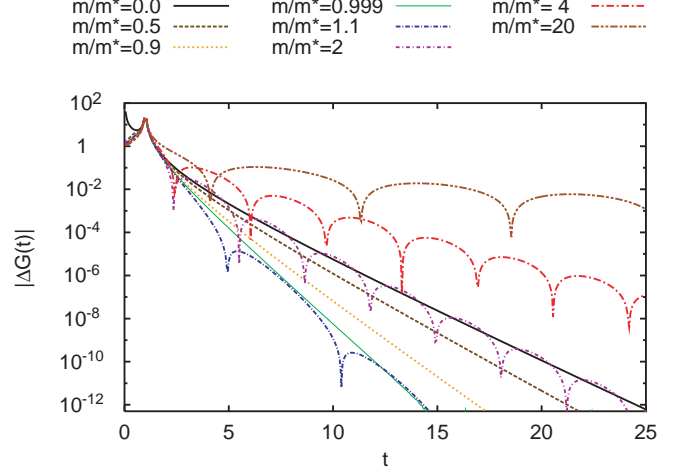


FIG. 6: (color online) Linear-log plots of the absolute value  $|\Delta G(t)|$  of the function  $\Delta G(t) = G(t) - 1 - \tau_r/(t - \tau_r)$  as a function of time  $t$  for the work done in the comoving frame in the case of a nonequilibrium steady state initial condition. Lines in these graphs correspond to parameter values of the scaled masses  $m/m^* = 0, 0.5, 0.9, 0.999, 1.1, 2, 4$  and  $20$  as indicated above this figure and we use the same parameter values  $\alpha$ ,  $\kappa$  and  $t_0$  as in Fig. 2.

1 in this frame should be close to that of the over-damped case.

Now, we discuss the time-oscillatory behavior of  $G(t)$  in the comoving frame. We note that in the comoving frame the approach of  $G(t)$  to its final value 1 is via oscillations around the over-damped line, contrary to in the laboratory frame where this approach is unrelated to the over-damped line. Such time-oscillations are already visible for large masses  $m \gg m^*$  in Fig. 5, but to show them in a more magnified way, we plotted in Fig. 6 the absolute value  $|\Delta G(t)|$  of the function  $\Delta G(t)$  defined by Eq. (61) as a function of time  $t$  as linear-log plots. Here, we plotted data for the scaled masses  $m/m^* = 0, 0.5, 0.9, 0.999, 1.1, 2, 4$  and  $20$  and for the time period  $t \in [0, 25]$ . It is shown in Fig. 6 that time-oscillations of  $\Delta G(t)$  occur for  $m/m^* > 1$  but not for  $0 \leq m/m^* < 1$ . Moreover,  $\Delta G(t)$  for  $0 \leq m/m^* < 1$  decays faster,

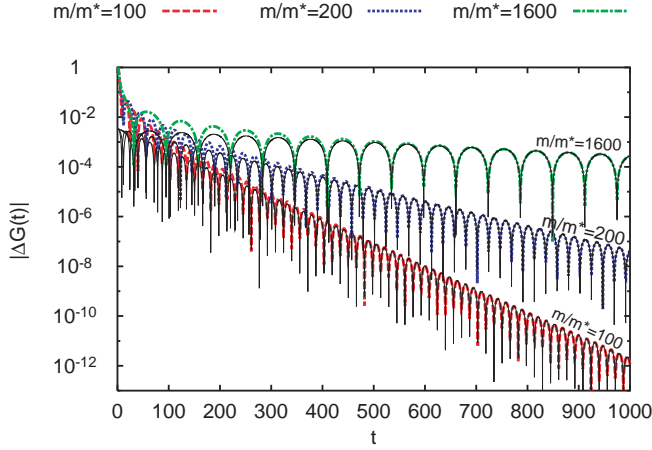


FIG. 7: (color online) Long time behavior of  $|\Delta G(t)|$  as a function of time  $t$  as linear-log plots for the work done in the comoving frame in the case of a nonequilibrium steady state initial condition. Here, we use the same parameter values  $\alpha$ ,  $\kappa$  and  $t_0$  as in Fig. 2. Broken, dotted and dash-dotted lines in these graphs correspond to parameter values of the scaled masses  $m/m^* = 100, 200$  and  $1600$ , respectively. Solid lines are fits of  $|\Delta G(t)|$  to the function (62) using Table I, and they are visually indistinguishable from the graphs of  $|\Delta G(t)|$  except for short times.

while  $\Delta G(t)$  for  $m/m^* > 1$  decays slower with time, for increasing mass. These features are similar to those in the laboratory frame.

In Fig. 7 we show linear-log plots of  $|\Delta G(t)|$  as functions of  $t$  for longer times  $t \in [0, 1000]$  and for larger masses  $m/m^* = 100, 200$  and  $1600$  than in Fig. 6. Comparing this figure in the comoving frame with the corresponding Fig. 4 in the laboratory frame, we can see that the time-oscillation amplitudes of the function  $\Delta G(t)$  in the comoving frame are much smaller than the corresponding ones in the laboratory frame, except for short times. This should be noted as an important frame-dependence in the behavior of  $G(t)$ .

The time-oscillation periods appearing in Figs. 6 and 7 can be checked by fitting the data again to the function (62) with the time-oscillation period (58). We only show such fitting lines for Fig. 7 using the fitting parameters  $a$ ,  $b$  and  $c$  of Table I. Like for the fitting lines in Fig. 4, the parameter values of  $a$  and  $b$  in Table I in the comoving frame also appear to vary non-negligibly for data for a longer time period than that shown in Fig. 7. Therefore, as for Fig. 4, the fitting lines in Fig. 7 should not be regarded as evidence for the exponential decay in the fitting function (62). However, the fits of their time-oscillation periods of  $|\Delta G(t)|$  to the function (62) in Fig. 7 are satisfactory, which suggests again that the time-oscillations of  $G(t)$  have the same origin as those in the position  $\hat{x}_s^*$ , like in the laboratory frame.

## VI. SUMMARY AND REMARKS

As a summary of this paper, we have discussed inertial effects related to the particle mass  $m$  in nonequilibrium work distribution functions and their associated fluctuation theorems for a dragged Brownian particle model confined by a harmonic potential using a path integral approach for all times: asymptotic as well as finite. We considered two kinds of work: the work  $\mathcal{W}_l$  done in the laboratory frame and the work  $\mathcal{W}_c$  done in the comoving frame and we calculated the distribution functions  $P_w(W, t)$  for them. Using the distributions for the work in the different frames we analytically proved, for any initial condition, an asymptotic work fluctuation theorem, which has the same form in both the frames. This contrasts with what happens for finite times, when for a nonequilibrium steady state initial condition there are major differences between the work fluctuations in the laboratory and comoving frames. This was discussed, using the quantity  $G(t) \equiv (\partial/\partial W) \ln[P_w(W, t)/P_w(-W, t)]$ , which approaches the value 1 in the long time limit  $t \rightarrow +\infty$  by the asymptotic fluctuation theorem. The  $G(t)$  for the work  $\mathcal{W}_c$  done in the comoving frame is larger than 1 at all times and converges to the corresponding over-damped value much before converging to its final value 1. On the other hand, the  $G(t)$  for the work  $\mathcal{W}_l$  done in the laboratory frame can be smaller than 1 for sufficiently large times and masses, and the relaxation behavior of  $G(t)$  to its final value 1 is very different from that for the over-damped case, even for long times. As one of the significant effects for finite times, we also discussed the existence of a critical mass  $m^*$ , so that for the mass  $m > m^*$  a time-oscillatory behavior appears in  $G(t)$  in both frames.

In the remainder of this section, we make some remarks on the contents in the main text of this paper.

1) We have discussed in this paper differences between the works  $\mathcal{W}_l$  and  $\mathcal{W}_c$ , which originate in a frame dependence of the kinetic energy difference due to the d'Alembert-like force as we discussed in Sec. III A. In contrast to the work and the kinetic energy difference, the heat (as well as the potential energy difference) is frame-independent even in the inertial case. Note that the two works  $\mathcal{W}_l$  and  $\mathcal{W}_c$  have the same average value in the nonequilibrium steady state, because their difference can be represented as a “boundary term”

$$\mathcal{W}_l - \mathcal{W}_c = m(\dot{x}_t - \dot{x}_{t_0})v \quad (63)$$

depending on a difference between the two boundary values of  $\dot{x}_s$  at the final time  $s = t$  and the initial time  $s = t_0$  only, so that the average of this boundary term  $m(\dot{x}_t - \dot{x}_{t_0})v$  is zero in the nonequilibrium steady state. Nevertheless, this difference  $m(\dot{x}_t - \dot{x}_{t_0})v$  between  $\mathcal{W}_l$  and  $\mathcal{W}_c$  causes dramatic differences in the work fluctuations, as shown in the subsections VB and VC of this paper.

2) In a different nonequilibrium model described by a linear Langevin equation, Ref. [16] considered the motion of a torsion pendulum under an external torque in a

Brownian particle	$x_s$	$m$	$\alpha$	$\kappa$	$\kappa v$
Torsion pendulum	$\theta_s$	$I$	$\nu$	$C$	$\mu$

TABLE II: Correspondences between the dragged Brownian particle model described by Eq. (3) and the torsion pendulum model described by Eq. (64).

fluid. The corresponding Langevin equation for the angular displacement  $\theta_s$  of the pendulum at time  $s$  in this system is then given by

$$I \frac{d^2 \theta_s}{ds^2} = -\nu \frac{d\theta_s}{ds} - C\theta_s + M_s + \zeta_s \quad (64)$$

where  $I$  is the total moment of inertia of the displaced mass,  $\nu$  is the viscous damping,  $C$  the elastic torsional stiffness of the pendulum,  $M_s$  the external torque, and  $\zeta_s$  the Gaussian-white random force. For this model, Ref. [16] considered the case of a linear torque of

$$M_s = \mu s \quad (65)$$

with a force constant  $\mu$ . It is important to note that Eq. (64) with the force (65) has mathematically the same form as the Langevin equation (3) with the correspondences shown in Table II. Based on these correspondences between the two models, for example, there should be a critical value  $I^*$  of the total moment of inertia above which a similar time-oscillatory behavior occurs in the pendulum model, like above the critical mass  $m^*$  in the dragged Brownian particle model treated in this paper.

For the pendulum system, Ref. [16] considered the work  $\mathcal{W}_p$  done by the external torque  $M_s$  on the pendulum ( $p$ ). This work is given there by

$$\mathcal{W}_p = \int_{t_0}^t ds (M_s - M_{t_0}) \frac{d\theta_s}{ds}. \quad (66)$$

Using Eq. (65) and the correspondences in Table II, this work corresponds to a quantity for our dragged Brownian particle model, viz.

$$\begin{aligned} \mathcal{W}_p &\longleftrightarrow \int_{t_0}^t ds \kappa v(s - t_0) \frac{dx_s}{ds} \\ &= \mathcal{W}_l + \kappa v(t - t_0) \left[ x_t - \frac{1}{2}v(t + t_0) \right] \end{aligned} \quad (67)$$

which is clearly different from the works  $\mathcal{W}_l$  and  $\mathcal{W}_c$  discussed in this paper. In other words,  $\mathcal{W}_l$ ,  $\mathcal{W}_c$  and  $\mathcal{W}_p$  give physically different kinds of work in nonequilibrium steady states described by a mathematically identical Langevin equation in a dynamical sense. We note that our  $\mathcal{W}_l$  and  $\mathcal{W}_c$  are consequences of the generalized Onsager-Machlup theory in Ref. [6]. We reserve a general discussion on fluctuation theorems for different kinds of work for a future publication.

3) As another nonequilibrium model described by a linear Langevin equation, Ref. [22] considered electric

circuit models. In that case the system is described by a first-order linear Langevin equation, which has the same form as the over-damped Langevin equation for the dragged Brownian particle model. As a generalization of these electric circuit models, an inertial effect in the electric circuit can be introduced by including its self-induction. A generalization of the arguments of Ref. [22] to the case including the self-induction, as well as a discussion of the effects of self-induction on the nonequilibrium work (and heat) fluctuations, will be addressed in a future paper. Especially, it would be interesting to observe whether there is a critical value of the self-induction, above which similar oscillatory effects occur, as appear above the critical mass in the inertial case in this paper.

4) The critical mass  $m^*$  discussed in this paper for work fluctuations also appears in the dynamics of the average position  $\langle x_s \rangle$ . In order to discuss this point, we note that taking the average of Eq. (3), the average position  $\langle x_s \rangle$  of the particle at time  $s$  satisfies

$$m \frac{d^2 \langle x_s \rangle}{ds^2} = -\alpha \frac{d\langle x_s \rangle}{ds} - \kappa (\langle x_s \rangle - vs) \quad (68)$$

using  $\langle \zeta_s \rangle = 0$ . Using  $\nu_{\pm}$  defined by Eq. (20), the solution of Eq. (68) is given by

$$\langle x_s \rangle = v(s - \tau_r) + C' e^{-\nu_+ s} + C'' e^{-\nu_- s} \quad (69)$$

where the constants  $C'$  and  $C''$  are determined by the average initial conditions  $\langle x_{t_0} \rangle$  and  $\langle \dot{x}_{t_0} \rangle$  and are given by

$$\begin{aligned} C' &= -\frac{\nu_- e^{\nu_+ t_0}}{\nu_+ - \nu_-} [\langle x_{t_0} \rangle - v(t_0 - \tau_r)] \\ &\quad - \frac{e^{\nu_+ t_0}}{\nu_+ - \nu_-} (\langle \dot{x}_{t_0} \rangle - v), \end{aligned} \quad (70)$$

$$\begin{aligned} C'' &= \frac{\nu_+ e^{\nu_- t_0}}{\nu_+ - \nu_-} [\langle x_{t_0} \rangle - v(t_0 - \tau_r)] \\ &\quad + \frac{e^{\nu_- t_0}}{\nu_+ - \nu_-} (\langle \dot{x}_{t_0} \rangle - v). \end{aligned} \quad (71)$$

Since the  $\nu_{\pm}$  include nonzero imaginary parts for  $m > m^*$ , a time-oscillatory behavior appears in the average position  $\langle x_s \rangle$  for masses above this critical mass  $m^*$ . This kind of phenomenon was discussed for a damped oscillator model [19], but its effect on fluctuations in a nonequilibrium steady state has not been discussed to the best of our knowledge.

In Ref. [6], we discussed that in the over-damped case, the most probable path, which is a solution of the Euler-Lagrange equation for the Lagrangian function in the Onsager-Machlup theory, is expressed as a combination of forward and backward paths. This is also true in the inertial case, in which the most probable path is given by a solution of the “Euler-Lagrange” equation (16) for  $\lambda = 0$ . To show this, we note that the exponentially decaying terms  $\exp(-\nu_+ s)$  and  $\exp(-\nu_- s)$  on the right-hand side of Eq. (69) refer to a forward path. We can also introduce the corresponding backward path, as a combination of exponentially divergent terms  $\exp(\nu_+ s)$  and  $\exp(\nu_- s)$ . A combination of these forward and backward paths gives then the most probable path  $\{x_s^*\}_{s \in [t_0, t]}$  for  $\lambda = 0$ , i.e. Eq. (18).

5) There is still the open question of an analytical discussion of the asymptotic form of  $\Delta G(t)$  with the time-oscillations shown in Figs. 3, 4, 6 and 7. In this paper we only analyzed  $\Delta G(t)$  numerically by fitting it to the function (62), but in principle, such analytical information on  $\Delta G(t)$  is contained in the general form (55) of  $G(t)$ .

6) We have considered the asymptotic fluctuation theorem for work in this paper. We now address very briefly its connection with other fluctuation theorems.

(6a) One of the other fluctuation theorems is the transient fluctuation theorem [2]. This fluctuation theorem was already derived and discussed for a dragged Brownian particle model with inertia in Ref. [6]. There, we derived transient fluctuation theorems, not only for the same works as those in this paper, but also for an energy loss by friction. Different from the work, the distribution function for the energy loss by friction does *not* satisfy an asymptotic fluctuation theorem.

(6b) Another important fluctuation theorem is the extended heat fluctuation theorem [20, 23]. In Ref. [6]

we gave a simple derivation of this fluctuation theorem, based on the assumptions that (A) a correlation between the work and the energy difference at time  $t$  (as well as a correlation between the energies at the initial time  $t_0$  and the final time  $t$ ) disappears in the long time limit  $t \rightarrow +\infty$ , (B) the work satisfies the asymptotic fluctuation theorem, (C) the work distribution function approaches a Gaussian distribution asymptotically in time, and (D) the distribution function  $P_e(E)$  for energy  $E$  is canonical-like, namely  $P_e(E) \approx \exp(-\beta E)$  for  $E > 0$ . The same derivation could be applied to all models which satisfy these four conditions (A), (B), (C) and (D). In particular, using this derivation, one can derive an analytical expression for the asymptotic heat distribution function itself, as well as the extended heat fluctuation theorem not only for the over-damped case, as was done in Ref. [6], but also for the inertial case.

### Acknowledgements

We gratefully acknowledge financial support of the National Science Foundation, under award PHY-0501315.

## APPENDIX A: ASYMPTOTIC PROPERTY FOR THE MATRIX $\Lambda_t$

In this Appendix we prove Eq. (46) for the matrix  $\Lambda_t$ . To show this equation in a simple way, without losing generality we take the origin of time at  $(t_0 + t)/2$  so that the initial time is given by  $t_0 = -t$ , only in this Appendix.

To consider the structure of the matrix  $\Lambda_t$  defined by Eq. (39) in the long time limit  $t \rightarrow +\infty$ , we first calculate the asymptotic form of the matrix  $\Gamma \Phi_t \Gamma$ , which is an essential element of the matrix  $\Lambda_t$ . For this purpose we note

$$\mathbf{K}_s \mathbf{K}_s^T = \begin{pmatrix} e^{2\nu_+ s} & e^{(\nu_+ + \nu_-)s} & e^{(\nu_+ - \nu_-)s} & 1 \\ e^{(\nu_+ + \nu_-)s} & e^{2\nu_- s} & 1 & e^{-(\nu_+ - \nu_-)s} \\ e^{(\nu_+ - \nu_-)s} & 1 & e^{-2\nu_- s} & e^{-(\nu_+ + \nu_-)s} \\ 1 & e^{-(\nu_+ - \nu_-)s} & e^{-(\nu_+ + \nu_-)s} & e^{-2\nu_+ s} \end{pmatrix}. \quad (\text{A.1})$$

Inserting Eq. (A.1) into Eq. (41) and using the relation  $t_0 = -t$  we obtain

$$\Phi_t = 2 \begin{pmatrix} \frac{\sinh(2\nu_+ t)}{2\nu_+} & \frac{\sinh[(\nu_+ + \nu_-)t]}{\nu_+ + \nu_-} & \frac{\sinh[(\nu_+ - \nu_-)t]}{\nu_+ - \nu_-} & t \\ \frac{\sinh[(\nu_+ + \nu_-)t]}{\nu_+ + \nu_-} & \frac{\sinh(2\nu_- t)}{2\nu_-} & t & \frac{\sinh[(\nu_+ - \nu_-)t]}{\nu_+ - \nu_-} \\ \frac{\sinh[(\nu_+ - \nu_-)t]}{\nu_+ - \nu_-} & t & \frac{\sinh(2\nu_- t)}{2\nu_-} & \frac{\sinh[(\nu_+ + \nu_-)t]}{\nu_+ + \nu_-} \\ t & \frac{\sinh[(\nu_+ - \nu_-)t]}{\nu_+ - \nu_-} & \frac{\sinh[(\nu_+ + \nu_-)t]}{\nu_+ + \nu_-} & \frac{\sinh(2\nu_+ t)}{2\nu_+} \end{pmatrix} \quad (\text{A.2})$$

with the hyperbolic function  $\sinh(x) \equiv [\exp(x) - \exp(-x)]/2$ . Equations (34) and (A.2) lead to

$$\Gamma \Phi_t \Gamma = \begin{pmatrix} \Psi_t & 0_2 \\ 0_2 & 0_2 \end{pmatrix} \quad (\text{A.3})$$

where  $0_2$  is the  $2 \times 2$  null matrix, and the  $2 \times 2$  matrix  $\Psi_t$  is given by

$$\begin{aligned}\Psi_t &\equiv 4 \begin{pmatrix} \nu_+ \sinh(2\nu_+ t) & \frac{2\nu_+ \nu_-}{\nu_+ + \nu_-} \sinh[(\nu_+ + \nu_-)t] \\ \frac{2\nu_+ \nu_-}{\nu_+ + \nu_-} \sinh[(\nu_+ + \nu_-)t] & \nu_- \sinh(2\nu_- t) \end{pmatrix} \\ &\stackrel{t \rightarrow +\infty}{\sim} 2 \begin{pmatrix} \nu_+ e^{2\nu_+ t} & \frac{2\nu_+ \nu_-}{\nu_+ + \nu_-} e^{(\nu_+ + \nu_-)t} \\ \frac{2\nu_+ \nu_-}{\nu_+ + \nu_-} e^{(\nu_+ + \nu_-)t} & \nu_- e^{2\nu_- t} \end{pmatrix} \\ &= 2 \begin{pmatrix} e^{\nu_+ t} & 0 \\ 0 & e^{\nu_- t} \end{pmatrix} \begin{pmatrix} \nu_+ & \frac{2\nu_+ \nu_-}{\nu_+ + \nu_-} \\ \frac{2\nu_+ \nu_-}{\nu_+ + \nu_-} & \nu_- \end{pmatrix} \begin{pmatrix} e^{\nu_+ t} & 0 \\ 0 & e^{\nu_- t} \end{pmatrix}. \end{aligned} \quad (\text{A.4})$$

Here, we used the positivity  $\text{Re}\{\nu_\pm\} > 0$  of the real part of  $\nu_\pm$  (assuming a nonzero mass  $m \neq 0$  and a nonzero spring constant  $\kappa \neq 0$ ) and also  $\sinh(at) \stackrel{t \rightarrow +\infty}{\sim} (1/2)\exp(at)$  for any number  $a$  with the positive real part  $\text{Re}\{a\} > 0$ .

Second, we obtain a simplified form of the matrix  $A_t^{-1}$  in the long time limit, which is another essential element of the matrix  $\Lambda_t$ . Noting again that the real part of the number  $\nu_\pm$  is (strictly non-zero) positive and the initial time is given by  $t_0 = -t$ , we obtain the asymptotic form of the matrix  $A_t$  defined by Eq. (25) as

$$A_t \stackrel{t \rightarrow +\infty}{\sim} \begin{pmatrix} 0_2 & A_t^{(1)} \\ A_t^{(2)} & 0_2 \end{pmatrix}. \quad (\text{A.5})$$

for the long time limit  $t \rightarrow +\infty$ . Here,  $0_2$  is the  $2 \times 2$  null matrix, and  $A_t^{(j)}$ ,  $j = 1, 2$  are defined by

$$A_t^{(1)} \equiv \begin{pmatrix} e^{\nu_- t} & e^{\nu_+ t} \\ -\nu_- e^{\nu_- t} & -\nu_+ e^{\nu_+ t} \end{pmatrix}, \quad (\text{A.6})$$

$$A_t^{(2)} \equiv \begin{pmatrix} e^{\nu_+ t} & e^{\nu_- t} \\ \nu_+ e^{\nu_+ t} & \nu_- e^{\nu_- t} \end{pmatrix}. \quad (\text{A.7})$$

From Eq. (A.5) we derive

$$A_t^{-1} \stackrel{t \rightarrow +\infty}{\sim} \begin{pmatrix} 0_2 & A_t^{(2)-1} \\ A_t^{(1)-1} & 0_2 \end{pmatrix} \quad (\text{A.8})$$

where  $A_t^{(1)-1}$  and  $A_t^{(2)-1}$  are given by

$$A_t^{(1)-1} = \frac{1}{\nu_- - \nu_+} \begin{pmatrix} -\nu_+ e^{-\nu_- t} & -e^{-\nu_- t} \\ \nu_- e^{-\nu_+ t} & e^{-\nu_+ t} \end{pmatrix}, \quad (\text{A.9})$$

$$A_t^{(2)-1} = \frac{1}{\nu_- - \nu_+} \begin{pmatrix} \nu_- e^{-\nu_+ t} & -e^{-\nu_+ t} \\ -\nu_+ e^{-\nu_- t} & e^{-\nu_- t} \end{pmatrix}. \quad (\text{A.10})$$

Eq. (A.8) give an asymptotic form for the matrix  $A_t^{-1}$ .

Finally, using Eqs. (39), (A.3) and (A.8) we obtain the asymptotic form of the matrix  $\Lambda_t$  as

$$\Lambda_t \stackrel{t \rightarrow +\infty}{\sim} \begin{pmatrix} 0_2 & 0_2 \\ 0_2 & [A_t^{(2)-1}]^T \Psi_t A_t^{(2)-1} \end{pmatrix}. \quad (\text{A.11})$$

Here, using Eqs. (A.4) and (A.10) the non-vanishing matrix elements of the matrix (A.11) is given by

$$\begin{aligned} [A_t^{(2)-1}]^T \Psi_t A_t^{(2)-1} &\stackrel{t \rightarrow +\infty}{\sim} 2 \begin{pmatrix} \frac{\nu_+ \nu_-}{\nu_+ + \nu_-} & 0 \\ 0 & \frac{1}{\nu_+ + \nu_-} \end{pmatrix} \\ &= \frac{2}{\alpha} \begin{pmatrix} \kappa & 0 \\ 0 & m \end{pmatrix} \end{aligned} \quad (\text{A.12})$$

where we used  $\nu_+ + \nu_- = \alpha/m$  and  $\nu_+ \nu_- = \kappa/m$ . By Eqs. (A.11) and (A.12) we obtain

$$\lim_{t \rightarrow +\infty} \Lambda_t = \frac{2}{\alpha} \begin{pmatrix} 0 & 0 & 0 & 0 \\ 0 & 0 & 0 & 0 \\ 0 & 0 & \kappa & 0 \\ 0 & 0 & 0 & m \end{pmatrix}. \quad (\text{A.13})$$

Equation (A.13) shows that the matrix  $\Lambda_t$  approaches a time-independent constant matrix in the long time limit  $t \rightarrow +\infty$ . Therefore, the matrix  $\Lambda_t/(t - t_0)$  approaches the  $4 \times 4$  null matrix in the long time limit  $t \rightarrow +\infty$ , implying that the condition (46) is satisfied.

## APPENDIX B: WORK DISTRIBUTION FOR THE NONEQUILIBRIUM STEADY STATE

In this Appendix we give a derivation of Eq. (52) for the work distribution function  $P(W, t)$  in the case of the nonequilibrium steady state initial condition (51).

First, we note that the initial distribution function (51) can be written in the form

$$f(x_i, p_i, t_0) = \frac{\beta}{2\pi} \sqrt{\frac{\kappa}{m}} \exp \left\{ -\frac{\alpha\beta}{4} [\mathbf{B}_{if}^{(1)}]^T \Lambda^{(0)} \mathbf{B}_{if}^{(1)} \right\}, \quad (\text{B.1})$$

using Eqs. (26) and (54). Equation (B.1) means that the initial distribution function  $f(x_i, p_i, t_0)$  is Gaussian for the components of the vector  $\mathbf{B}_{if}^{(1)}$ . Using Eq. (B.1) and again the vector  $\mathbf{B}_{if}^{(1)}$  given by Eq. (26), the work distribution function (44) can be represented by

$$P_w(W, t) = \frac{C_\varepsilon m \beta}{4\pi v} \sqrt{\frac{\kappa m}{\pi \alpha \beta (t - t_0 - \tau_r^2 \mathbf{J}^T \Lambda_t \mathbf{J})}} \int \int \int \int d\mathbf{B}_{if}^{(1)} \times \exp \left\{ -\frac{1}{4} \alpha \beta [\mathbf{B}_{if}^{(1)}]^T (\Lambda^{(0)} + \Lambda_t) \mathbf{B}_{if}^{(1)} - \frac{[\alpha \beta v (\boldsymbol{\eta}^T - \tau_r \mathbf{J}^T \Lambda_t) \mathbf{B}_{if}^{(1)} - W + \alpha \beta v^2 (t - t_0)]^2}{4 \alpha \beta v^2 (t - t_0 - \tau_r^2 \mathbf{J}^T \Lambda_t \mathbf{J})} \right\} \quad (\text{B.2})$$

where we used the relation  $dx_i dp_i dx_f dp_f = m^2 d\mathbf{B}_{if}^{(1)}$  because of Eq. (26).

Now, we note that

$$\begin{aligned} (\tilde{\mathbf{a}}^T \tilde{\mathbf{x}} + \tilde{b})^2 + \tilde{\mathbf{x}}^T \tilde{\mathcal{C}} \tilde{\mathbf{x}} &= \tilde{\mathbf{x}}^T (\tilde{\mathbf{a}} \tilde{\mathbf{a}}^T + \tilde{\mathcal{C}}) \tilde{\mathbf{x}} + 2 \tilde{b} \tilde{\mathbf{a}}^T \tilde{\mathbf{x}} + \tilde{b}^2 \\ &= \left[ \tilde{\mathbf{x}} + \tilde{b} (\tilde{\mathbf{a}} \tilde{\mathbf{a}}^T + \tilde{\mathcal{C}})^{-1} \tilde{\mathbf{a}} \right]^T (\tilde{\mathbf{a}} \tilde{\mathbf{a}}^T + \tilde{\mathcal{C}}) \left[ \tilde{\mathbf{x}} + \tilde{b} (\tilde{\mathbf{a}} \tilde{\mathbf{a}}^T + \tilde{\mathcal{C}})^{-1} \tilde{\mathbf{a}} \right] + \tilde{b}^2 \left[ 1 - \tilde{\mathbf{a}}^T (\tilde{\mathbf{a}} \tilde{\mathbf{a}}^T + \tilde{\mathcal{C}})^{-1} \tilde{\mathbf{a}} \right] \end{aligned} \quad (\text{B.3})$$

for any  $n$ -dimensional vector  $\tilde{\mathbf{a}}$  and  $\tilde{\mathbf{x}}$ , any scalar  $\tilde{b}$ , and any  $n \times n$  symmetric matrix  $\tilde{\mathcal{C}}$  existing the inverse matrix of  $\tilde{\mathbf{a}} \tilde{\mathbf{a}}^T + \tilde{\mathcal{C}}$ . Applying Eq. (B.3) to Eq. (B.2) for the case of  $\tilde{\mathbf{x}} = \mathbf{B}_{if}^{(1)}$ ,  $\tilde{\mathbf{a}} = \alpha \beta v (\boldsymbol{\eta} - \tau_r \Lambda_t \mathbf{J})$ ,  $\tilde{b} = \alpha \beta v^2 (t - t_0) - W$  and  $\tilde{\mathcal{C}} = (\alpha \beta v)^2 (t - t_0 - \tau_r^2 \mathbf{J}^T \Lambda_t \mathbf{J}) (\Lambda^{(0)} + \Lambda_t)$ , and carrying out the integral over  $\mathbf{B}_{if}^{(1)} (= \tilde{\mathbf{x}})$  in Eq. (B.2), we obtain

$$\begin{aligned} P_w(W, t) &= \frac{C_\varepsilon m \beta}{4\pi v} \sqrt{\frac{\kappa m}{\pi \alpha \beta (t - t_0 - \tau_r^2 \mathbf{J}^T \Lambda_t \mathbf{J})}} \int \int \int \int d\tilde{\mathbf{x}} \exp \left\{ -\frac{(\tilde{\mathbf{a}}^T \tilde{\mathbf{x}} + \tilde{b})^2 + \tilde{\mathbf{x}}^T \tilde{\mathcal{C}} \tilde{\mathbf{x}}}{4 \alpha \beta v^2 (t - t_0 - \tau_r^2 \mathbf{J}^T \Lambda_t \mathbf{J})} \right\} \\ &= C'_w \exp \left\{ -\frac{\left[ 1 - \tilde{\mathbf{a}}^T (\tilde{\mathbf{a}} \tilde{\mathbf{a}}^T + \tilde{\mathcal{C}})^{-1} \tilde{\mathbf{a}} \right] \tilde{b}^2}{4 \alpha \beta v^2 (t - t_0 - \tau_r^2 \mathbf{J}^T \Lambda_t \mathbf{J})} \right\} \\ &= C'_w \exp \left\{ -\frac{1 - \Omega_t}{4 \alpha \beta v^2 (t - t_0 - \tau_r^2 \mathbf{J}^T \Lambda_t \mathbf{J})} [W - \alpha \beta v^2 (t - t_0)]^2 \right\} \end{aligned} \quad (\text{B.4})$$

using a normalization constant  $C'_w$  and Eq. (53) for  $\Omega_t$ . The constant  $C'_w$  in Eq. (B.4) can be determined by the normalization condition  $\int dW P(W, t) = 1$ , which and Eq. (B.4) yield Eq. (52).

### APPENDIX C: ASYMPTOTIC FORM OF $G(t)$

In this Appendix we give an argument to derive Eq. (56) for  $G(t)$ .

The essential point to derive Eq. (56) for  $G(t)$  is the asymptotic form (A.13), or equivalently

$$\lim_{t \rightarrow +\infty} \Lambda_t = 2 \begin{pmatrix} 0 & 0 & 0 & 0 \\ 0 & 0 & 0 & 0 \\ 0 & 0 & 1/\tau_r & 0 \\ 0 & 0 & 0 & \tau_m \end{pmatrix} \quad (\text{C.1})$$

using the relations  $\tau_r = \alpha/\kappa$  and  $\tau_m = m/\alpha$ . Using Eqs. (40), (45), (54) and (C.1) we obtain

$$\lim_{t \rightarrow +\infty} \mathbf{J}^T \Lambda_t \mathbf{J} = 2/\tau_r, \quad (\text{C.2})$$

$$\lim_{t \rightarrow +\infty} (\boldsymbol{\eta} - \tau_r \Lambda_t \mathbf{J}) = \begin{pmatrix} -1 \\ -\tau_m \vartheta \\ -1 \\ \tau_m \vartheta \end{pmatrix}, \quad (\text{C.3})$$

$$\lim_{t \rightarrow +\infty} (\Lambda^{(0)} + \Lambda_t) = 2 \begin{pmatrix} 1/\tau_r & 0 & 0 & 0 \\ 0 & \tau_m & 0 & 0 \\ 0 & 0 & 1/\tau_r & 0 \\ 0 & 0 & 0 & \tau_m \end{pmatrix} \quad (\text{C.4})$$

Equations (C.2), (C.3) and (C.4) lead to

$$\left[ (\boldsymbol{\eta} - \tau_r \Lambda_t \mathbf{J}) (\boldsymbol{\eta} - \tau_r \Lambda_t \mathbf{J})^T + (t - t_0 - \tau_r^2 \mathbf{J}^T \Lambda_t \mathbf{J}) (\Lambda^{(0)} + \Lambda_t) \right]^{-1} \\ \xrightarrow{t \rightarrow +\infty} \frac{\tau_r}{2(t - t_0 - 2\tau_r) \Xi_t} \begin{pmatrix} \Xi_t - \tau_r & -\vartheta & -\tau_r & \vartheta \\ -\vartheta & \frac{\Xi_t - \tau_r \vartheta^2}{\tau_r \tau_m} & -\vartheta & \frac{\vartheta^2}{\tau_r} \\ -\tau_r & -\vartheta & \Xi_t - \tau_r & \vartheta \\ \vartheta & \frac{\vartheta^2}{\tau_r} & \vartheta & \frac{\Xi_t - \tau_r \vartheta^2}{\tau_r \tau_m} \end{pmatrix} \quad (\text{C.5})$$

with  $\Xi_t \equiv 2(t - t_0 - \tau_r + \vartheta^2 \tau_m)$ . By Eqs. (53), (C.3) and (C.5), we obtain

$$\Omega_t \xrightarrow{t \rightarrow +\infty} \frac{\tau_r + \tau_m \vartheta^2}{t - t_0 - \tau_r + \tau_m \vartheta^2}. \quad (\text{C.6})$$

From Eqs. (55), (C.2) and (C.6) we derive Eq. (56).

- 
- [1] D. J. Evans, E. G. D. Cohen, and G. P. Morriss, Phys. Rev. Lett. **71**, 2401 (1993); **71**, 3616 (1993) [errata].
  - [2] D. J. Evans and D. J. Searles, Phys. Rev. E **50**, 1645 (1994).
  - [3] G. Gallavotti and E. G. D. Cohen, Phys. Rev. Lett. **74**, 2694 (1995); J. Stat. Phys. **80**, 931 (1995).
  - [4] J. Kurchan, J. Phys. A: Math. Gen. **31**, 3719 (1998).
  - [5] J. L. Lebowitz and H. Spohn, J. Stat. Phys. **95**, 333 (1999).
  - [6] T. Taniguchi and E. G. D. Cohen, J. Stat. Phys. **126**, 1 (2007).
  - [7] L. Onsager and S. Machlup, Phys. Rev. **91**, 1505 (1953).
  - [8] S. Machlup and L. Onsager, Phys. Rev. **91**, 1512 (1953).
  - [9] S. Ciliberto and C. Laroche, J. Phys. IV France **8**, 215 (1998).
  - [10] G. M. Wang, E. M. Seveck, E. Mittag, D. J. Searles, and D. J. Evans, Phys. Rev. Lett. **89**, 050601 (2002).
  - [11] X.-D. Shang, P. Tong, and K.-Q. Xia, Phys. Rev. E **72**, 015301R (2005).
  - [12] S. Schuler, T. Speck, C. Tietz, J. Wrachtrup, and U. Seifert, Phys. Rev. Lett. **94**, 180602 (2005).
  - [13] G. Gallavotti, Phys. Rev. Lett. **77**, 4334 (1996); G. Gallavotti and D. Ruelle, Commun. Math. Phys. **190**, 279 (1997).
  - [14] E. G. D. Cohen and G. Gallavotti, J. Stat. Phys. **96**, 1343 (1999).
  - [15] F. Zamponi, F. Bonetto, L. F. Cugliandolo, and J. Kurchan, J. Stat. Mech. P09013 (2005).
  - [16] F. Douarche, S. Joubaud, N. B. Garnier, A. Petrosyan, and S. Ciliberto, Phys. Rev. Lett. **97**, 140603 (2006); S. Joubaud, N. B. Garnier, S. Ciliberto, e-print cond-mat/0703798.
  - [17] H. Risken, *The Fokker-Planck equation: methods of solution and applications* (Springer-Verlag, Berlin, 1989).
  - [18] D. J. Evans and G. P. Morriss, *Statistical mechanics of nonequilibrium liquids* (Academic Press, New York, 1990).
  - [19] L. D. Landau and E. M. Lifshitz, *Mechanics*, translated from the Russian by J. B. Sykes and J. S. Bell (Pergamon Press, Oxford, 1960).
  - [20] R. van Zon and E. G. D. Cohen, Phys. Rev. Lett. **91**, 110601 (2003); Phys. Rev. E **69**, 056121 (2004).
  - [21] R. van Zon and E. G. D. Cohen, Phys. Rev. E **67**, 046102 (2003).
  - [22] R. van Zon, S. Ciliberto, and E. G. D. Cohen, Phys. Rev. Lett. **92**, 130601 (2004).
  - [23] F. Bonetto, G. Gallavotti, A. Giuliani, and F. Zamponi, J. Stat. Phys. **123**, 39 (2006).
  - [24] A fluctuation theorem for a nonequilibrium steady state initial condition has been called the steady state fluctuation theorem (or the Gallavotti-Cohen fluctuation theorem [3]), which is a special case of asymptotic fluctuation theorems.
  - [25] The parameter  $\vartheta$  in Eq. (8) is chosen in a way consistent to that in our previous paper [6].
  - [26] In Ref. [6] we called only the first term on the right-hand side of Eq. (14) the Lagrangian function in the Onsager-Machlup theory, which is directly connected to a transition probability.
  - [27] In this paper,  $X^T$  means the transposed matrix (or vector) of any matrix (or vector)  $X$ .
  - [28] A function like  $\tilde{G}(W, t) \equiv (1/\langle W \rangle) \ln[P_w(W, t)/P_w(-W, t)]$  with the average work  $\langle W \rangle$  has been used to characterize fluctuation theorems [20]. The function (49) is connected to  $\tilde{G}(W, t)$  by  $G(W, t) = \langle W \rangle \partial \tilde{G}(W, t) / \partial W$ . One of the advantage to use  $G(W, t)$  instead of  $\tilde{G}(W, t)$  is that different from  $\tilde{G}(W, t)$ ,  $G(W, t)$  is independent of  $W$  when the distribution function  $P_w(W, t)$  is Gaussian, as shown in Eq. (52).
  - [29] Note that the work distribution function (59) approaches the distribution function (47) in the long time limit  $t \rightarrow +\infty$  because of  $t - t_0 - \tau_r(1 - b_t) \xrightarrow{t \rightarrow +\infty} t - t_0$ .
  - [30] We note that in this subsection we use the function (61) for  $\vartheta = 1$ , while in the next subsection VC we use the function (61) for  $\vartheta = 0$ .